2013-01-01

# Evaluation of Novel Backwashable Cartridge Filters: Efficacy and Sustainability

Michelle Brown
*University of Texas at El Paso*, mbrown5418@gmail.com

# EVALUATION OF NOVEL BACKWASHABLE CARTRIDGE FILTERS: EFFICACY AND SUSTAINABILITY

MICHELLE RENEE BROWN

Department of Civil Engineering

APPROVED:

W. Shane Walker, Ph.D., P.E., Chair

Thomas A. Davis, Ph.D.

Stephen W. Stafford, Ph.D.

Benjamin C. Flores, Ph.D.
Dean of the Graduate School

# Dedication

*To my Mom, Dad, and Brother.*
*Thank you for always supporting me in my studies and encouraging me to reach my goals.*

# EVALUATION OF NOVEL BACKWASHABLE CARTRIDGE FILTERS: EFFICACY AND SUSTAINABILITY

by

MICHELLE RENEE BROWN, B.S. MME

THESIS

Presented to the Faculty of the Graduate School of

The University of Texas at El Paso

in Partial Fulfillment

of the Requirements

for the Degree of

MASTER OF SCIENCE IN ENVIRONMENTAL ENGINEERING

Department of Civil Engineering

THE UNIVERSITY OF TEXAS AT EL PASO

May 2013

## Acknowledgements

I would like to thank Dr. Walker, my graduate advisor, and Dr. Stafford, my undergraduate advisor, for their guidance and words of encouragement. The dedication you both have for teaching is inspiring. You have taught me to think beyond the box. I also want to thank Dr. Davis, CIDS Director, for allowing me to contribute to the CIDS team and grow as a research student. I would like to thank those who allowed me to test the backwashable filter design. Without your development and constant cooperation, this project would not have been possible. I would also like to thank Dr. Lawler and Ijung Kim from UT Austin for being so welcoming and for taking time to instruct me on analysis procedures for the MS4; I am very grateful for all of your help. I would like to thank my fellow CIDS members who were always supportive. In particular I want to thank Chris Juarez, for his dedication to construct the test system; Isaac Campos, for standing in last minute to help run experiments; Jesse Valles, for answering all my plumbing questions; and Noe Ortega for helping out when pump problems arose. Finally, I would like to thank Malynda Cappelle, CIDS Associate Director, for choosing me to work on this project. I have learned so much from you over the past year and will always hold the memories of working together close to my heart.

# Abstract

One of the important aspects of desalination pre-treatment is the removal of particles from feedwater. This is typically accomplished using a combination of gross filtration and cartridge filtration. Cartridge filters are typically single-use products, and their replacement can represent a significant portion of a desalination plant's operating budget. This research evaluated the performance of a new type of cartridge filter that is backwashable and aims to reduce the overall cost to desalination facilities and provide cleaner water. Two sets of filters were evaluated (in triplicate) with respect to particle removal efficiency and hydraulic efficiency. The initial set included four types of cartridge filters that vary in geometry (size and layers), wall thickness (0.5-1.7 cm), and average pore size (15, 20, and 25 µm). The second set were second generation filters that were modified to improve hydraulic performance. The water being filtered was finished water from the El Paso Water Utility's Kay Bailey Hutchison (KBH) desalination plant with ground silica as the source of particles. Particle removal efficiency was evaluated by turbidity, as well as particle size distribution analysis using a Multisizer 4 Coulter Counter. Particle removal efficiency, which ranged from 94% to greater than 99%, was observed to be slightly sensitive to the reported average pore size. Second-generation filters showed consistency between filter triplicates, as well as varying degrees of filtrate particle reduction as a function of filter dimensions. Consistency in the Cartridge Filter Fouling Index (CFFI) was observed between backwashes, up to four consecutive backwashes (i.e., maximum tested). The second set of filters showed significant improvement in specific flux while maintaining superior filtrate particle reduction in comparison to the control cartridge filters.

# Table of Contents

# List of Tables

# List of Figures

# Chapter 1: Introduction

Both brackish water desalination and seawater desalination (including membrane and thermal systems) are becoming more common. The worldwide total desalination cumulative capacity, increased rapidly in the past several decades, as shown in Figure 1.1 (Gleick, 2006). According to Global Water Intelligence (GWI), there were more than 16,000 desalination plants worldwide with a production capacity of nearly 75,700 $m^3$/d in 2012 (GWI, 2012). This growth in desalination capacity over the decades can be attributed to advances in reverse osmosis (RO) membrane technology, reductions in desalination costs, and a continually increasing water demand (Tsiourtis, 2001; Zhou and Tol, 2005).

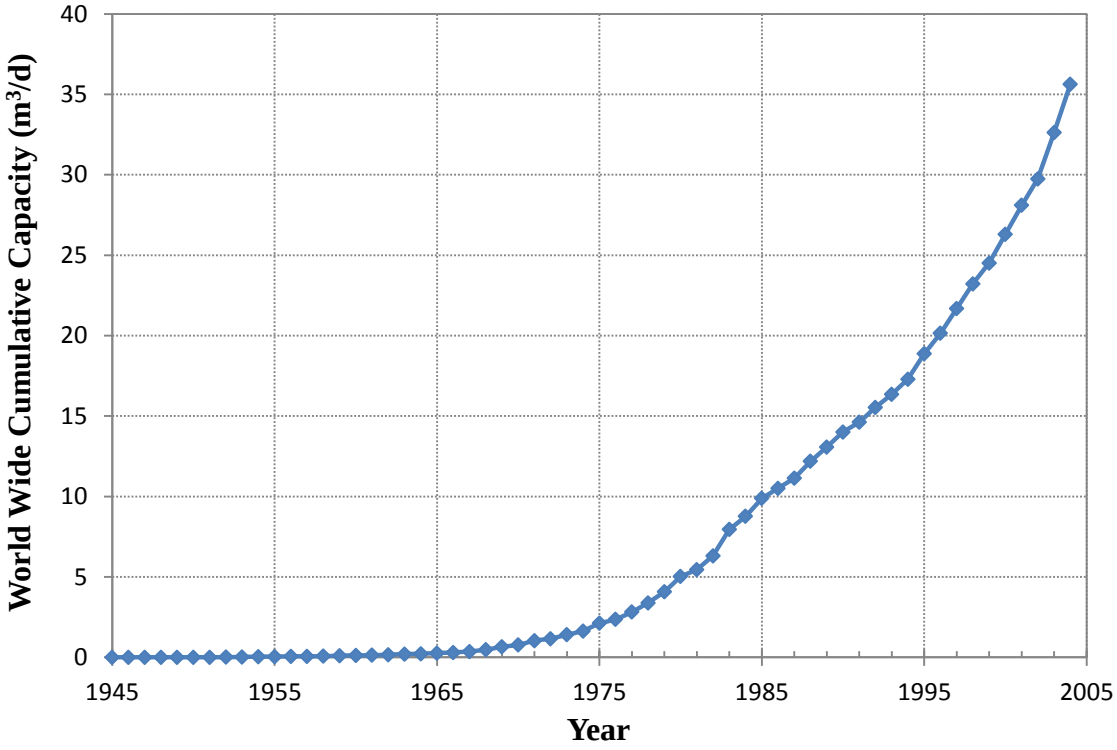


Figure 1.1 Global Cumulative Desalination Capacity

In addition to improvements in RO membrane technology, research of desalination pre-treatment processes has increased with hopes of lowering energy and cost while maintaining the quality of the feedwater heading to RO membranes. The primary purpose of pre-treatment is to improve the effectiveness and extend useful life of RO membranes by reducing particle concentration and

obstructing organic matter, which could lead to rapid fouling of the membranes. Pre-treatment also assists in decreasing overall treatment costs by reducing RO membrane replacement and cleaning frequency.

There are two forms of pre-treatment used to reduce particle concentration ahead of RO membrane processes: chemical and physical. Chemical pre-treatment uses scale inhibitors, coagulants, and other chemicals to minimize particle concentration. Both physical pre-treatment methods involve filtration: the conventional coagulation-flocculation-sedimentation-filtration water treatment process and media filtration (MF, NF, and UF filters). Cartridge filtration, as shown in Figure 1.2, can be included at the end of either method to serve as a final barrier for RO membrane protection in case the pretreatment method fails or leaks. Although cartridge filters are effective in protecting the RO membranes, they are typically not re-useable. This disadvantage leads to increased operator involvement, as well as an increase in waste and filter replacement costs. (Fritzmann, Lowenberg, Wintgens, & Melin, 2007)

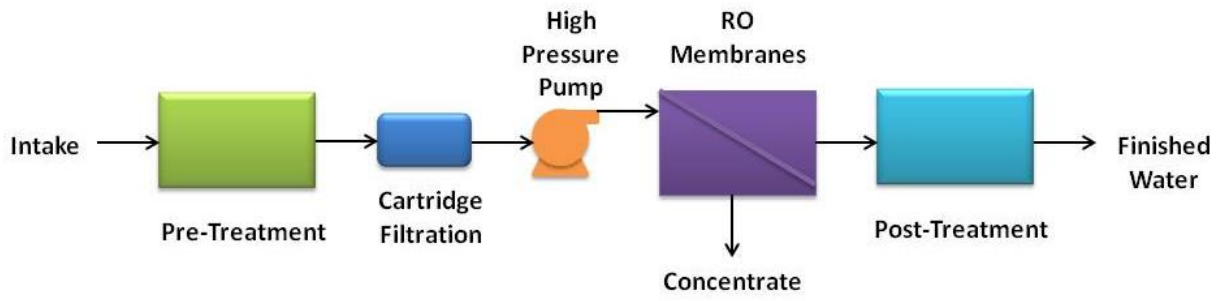


Figure 1.2 RO Desalination Plant Schematic

This research study evaluated several re-useable, backwashable cartridge filters with respect to filter efficacy and sustainability. The new filter design aims to provide cleaner water, reduce maintenance and waste, and lower the overall cost of treatment by reducing the frequency of filter replacement. A small pilot demonstration with laboratory analyses was performed to evaluate several backwashable filter designs.

## 1.1 Background – Membrane Desalination Pre-Treatment

Along coastal regions or inland locations where fresh water is scarce, brackish and seawater desalination by RO processes continue to grow around the world to meet the growing water demand

(Fritzmann, Lowenberg, Wintgens, & Melin, 2007). Seawater and brackish water can contain a high concentration of particles that can clog spiral-wound membrane modules or foul or damage RO membranes. This concentration is often monitored using turbidity.

Turbidity is measured in nephelometric turbidity units (NTU) and is based on the amount of light-scatter produced when light is aimed at a sample of particles suspended in water (Wilf & Bartels, 2006). Seawater turbidity fluctuates seasonally and can range from 2 to more than 200 NTU (Desormeaux, 2009; Voutchkov, 2010). Table 1.1 depicts typical turbidities by season:

Table 1.1 Sea Water Turbidity Range

| **Season** | | **Turbidity (NTU)** |
|---|---|---|
| Typical | March to Aug. | 3 |
| Red Tide Season | Sept. to Dec. | 2.5 |
| Storm Season | Nov. to March | 2-50 |

*Source: (Desormeaux, 2009)

Pre-treatment methods can effectively reduce the raw feedwater turbidity down to 0.5 NTU or lower before the water comes into contact with the RO membranes (Fritzmann, Lowenberg, Wintgens, & Melin, 2007). This, in turn, can prevent RO membrane fouling and extend membrane life (Fritzmann, Lowenberg, Wintgens, & Melin, 2007). Most RO membrane manufacturer's warranty the performance of their membranes based on several factors including feedwater turbidity (typically 0.5-0.1 NTU) (Bonnelye, Sanz, Durand, Plasse, Gueguen, & Mazounie, 2004) and Silt Density Index (typically less than 3-5) (Bonnelye, et al., 2004; Bu-Rashid and Czolkoss, 2007; Fritzmann, et al., 2007; Rybar, et al., 2005).

The Silt Density Index (SDI) is a parameter often used to characterize the particle fouling potential of a water (Fritzmann, Lowenberg, Wintgens, & Melin, 2007) but does not share a linear correlation with turbidity (Greenlee, Lawler, Freeman, Marrot, & Moulin, 2009). The method for calculating SDI is described by ASTM standard D4189-07 as how quickly clogging occurs when water is passed through a 0.45 μm microfiltration membrane at a constant pressure of 30 psi (ASTM, 2007).

The Modified Fouling Index is also a parameter used to characterize the fouling potential of a water. Schippers and Verdouw (1980) developed the Modified Fouling Index from the SDI based on gel filtration. It is measured using the same setup as SDI, except the volume of water filtered is recorded every 30 seconds for a total period of 20 minutes (Fritzmann, Lowenberg, Wintgens, & Melin, 2007). Boerlage and others (1997) have discussed the lack of correlation between SDI or the Modified Fouling Index and colloidal fouling.

Another parameter, not to be confused with the Modified Fouling Index, is the Membrane Fouling Index (MFI). The MFI is typically used as a point of comparison of the rate of fouling between filters in pilot experiments and is considered applicable when fouling resistance is proportional to specific throughput (volume of water filtered per membrane area). It is calculated by obtaining flux data from the experiment and performing either linear regression or determining the slope between two data points. (MWH, 2012, p. 869)

### 1.1.1 Cartridge Filters for RO Pre-treatment Application

The current market for cartridge filters is growing rapidly. Applications extend from inkjet printing to micro electronic component manufacturing and are the most common filtration method used to reduce particle concentrations of various liquids to the desired level. Widespread use occurred without standardized testing procedures for cartridge filters and has resulted in obscurity in filter performance ratings. This ambiguity amplifies the importance in relating filter testing and rating procedures to consumers. (Peuchot, Petillon, & Lynch, 2008)

Although cartridge filters are used in many industries and their applications vary, they are generally cylindrical in shape with their length depending on the respective housing size. They are made with various materials such as Polypropylene, High Density and Ultra High Molecular Weight Polyethylene, Polyester, Fiberglass, Cellulose, and sometimes Metal (Buehner, 2009; Porex, 2013). The most common types of cartridge filters are spun wound (Sutherland, 2009).

In RO pre-treatment, cartridge filter use is primarily aimed at extending RO membrane life. The filters are a last form of defense against RO membrane fouling and module clogging. Cartridge filters for pre-treatment applications are generally single-use, rated from 5 to 50 µm, and can be used in series.

Cartridge filter testing procedures for water treatment have been described by C.J. Williams and others (Williams, 1992; Bentley and Lloyd 1992; Peuchot et. al, 1994; Williams and Edyvean 1995; Williams and Edyvean 1996; and Williams 1997) in the 1990s. Testing involved the preparation of a slurry consisting of filtered water and Air Cleaner Coarse Test Dust (ACCTD) or Air Cleaner Fine Test Dust (ACFTD); these are also commonly referred to as Arizona Road Dust (Vijlee, 2002). Williams' 1992 paper prepared slurries with 1.75 g/L of ACCTD or ACFTD and evaluated 1-10 micron cotton fiber cartridge filters. Jourdan evaluated four types of cartridge filters and chose concentrations that would allow run times to be within 6 hours (Jourdan, Peuchot, & Hunt, 1994). The particle counter he used required concentrations less than 10 mg/L, so he had to alternate between 100 mg/L and 5 mg/L concentrations of ACFTD. The methodology used by both Jourdan and Williams was based on a withdrawn standard from the International Organization for Standardization (ISO), ISO 4572:1981 (ISO, 1981), which was a method for testing for particulates in hydraulic fluid. This method has been replaced with ISO 16889:2008 (ISO, 2008).

### 1.1.2 Economics

RO plant costs are dependent on several factors, which include type of feedwater, plant size, energy source and pre-treatment method. Typical plant costs can be broken up into three categories. First are energy costs for operation and maintenance, which comprise 50% of total costs. Next follows fixed costs, which account for about 40%. The last 10% goes towards maintenance, parts, membrane replacement, labor and chemicals. (Moran, Schreiber, Skelly, and Volpe, 2010, p.4)

The high cost for RO membrane replacement exceeds that of cartridge filtration replacement, which makes cartridge filters an advantageous media for pre-treatment. Although more cost effective than RO membranes, cartridge filters can easily clog/plug especially in applications where turbidities can widely vary.

The cost of cartridge filters can range between $100 to $300 per filter. At the Kay Bailey Hutchison desalination plant in El Paso, Texas (currently the largest inland brackish ground water reverse osmosis plant in the United States), costs for annual cartridge filter replacement alone can reach $250,000 when filters are replaced monthly. (Cappelle and Ruiz, personal communication, 2012)

### 1.1.3 Challenge

Considering the importance of the pretreatment function of providing reliable water quality, as well as the significant operating cost of replacing cartridge filters, there is the need to:

- Provide cleaner water than conventional cartridge filters
- Reduce waste
- Reduce down-time and maintenance

## 1.2 Goals and Objectives

The goal of this research is to investigate the efficacy and sustainability of a set of novel backwashable cartridge filters. The first objective of this research is to analyze the sensitivity of particle reduction and repeatability in performance after backwashing to physical attributes of prototype filters, such as geometry and nominal pore size. The second objective is to evaluate the performance of second-generation prototypes, based on results from the first objective. The third objective is to qualitatively evaluate the sustainability of these backwashable filters with respect to hydraulic performance in comparison to conventional cartridge filtration.

# Chapter 2: Materials and Methods

Pilot testing was conducted at the Consortium for High Tech Investigations of Water and Wastewater (CHIWAWA) laboratory located inside the KBH desalination plant in El Paso, TX. The plant was built as a joint effort between El Paso Water Utilities (EPWU) and Ft. Bliss, and the laboratory facility was made available by CHIWAWA members: EPWU, The University of Texas at El Paso (UTEP), New Mexico State University (NMSU), Agrilife at Texas A&M (TAMU), and the City of Alamogordo (El Paso Water Utilities, 2007). The laboratory has access to RO feed, concentrate, permeate, and finished water from KBH for research purposes. Finished water was used for conducting the laboratory-scale evaluation.

## 2.1 Apparatus

The filter testing system was constructed at the Center for Inland Desalination Systems (CIDS) Lab at The University of Texas at El Paso and transported to KBH for testing. It is composed of three skids (pump/manifold skid and two filter test skids) and two feed tanks (Figure 2.1). A 1500 gallon tank was used to supply a controlled silica slurry (KBH finished water mixed with ground silica test dust) to both skids for filter efficiency testing. A 250 gallon tank was used to feed KBH finished water to the test skid for the backwashing and clean water tests. A sump pump was connected and placed at the bottom center of the 1500 gallon feed tank to provide mixing of the slurry inside the tank to minimize settling/clarification.

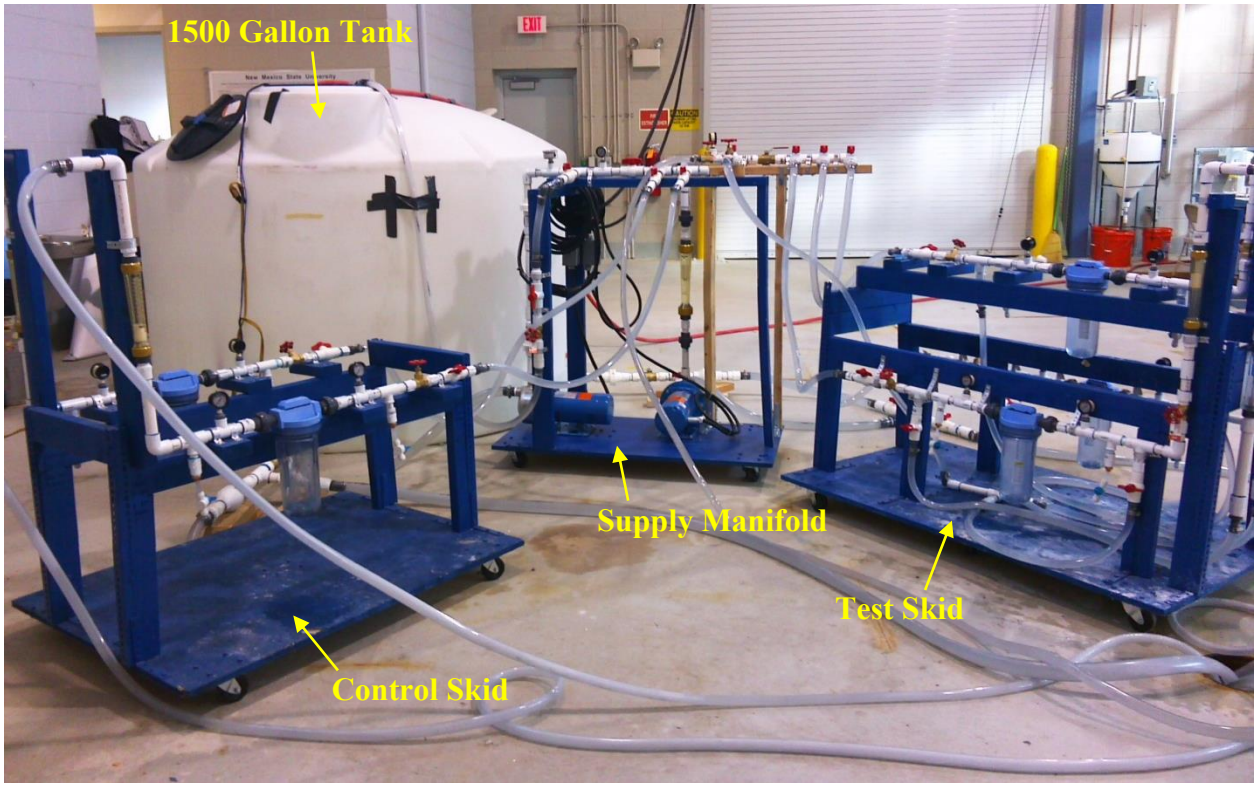


Figure 2.1 Filter Testing System Setup

The pump/supply manifold skid supports two separate manifolds. The first manifold directs flow to the control filter skid (Control Skid) which can simultaneously test two control cartridge filters. The second manifold directs flow to the backwashable filter test skid (Test Skid) which can simultaneously test or backwash three cartridge filters. To protect the pumps from cavitating, some of the flow was re-circulated back to the feed tank. The two filter housings on the control skid are referred to as positions 1 and 2 while the three housings on the backwashable filter skid are positions 3, 4, and 5. Figure 2.2 shows the layout of each test skid.

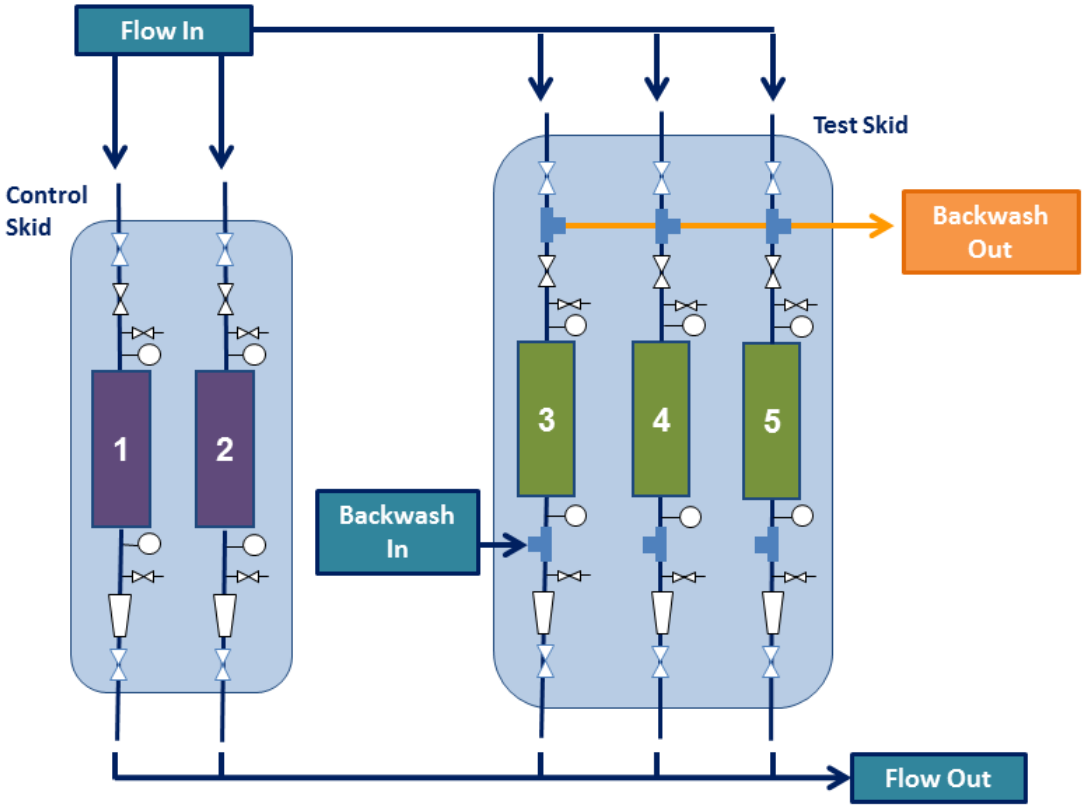


Figure 2.2 Control and Test Skid Schematic

### 2.1.1 Control Filters

Each experiment performed was tested against a 5 µm and 20 µm GE Hytrex Cartridge filter (control filters) on the control skid. These two GE filters are basic depth cartridge filters and were chosen because GE is one of the main suppliers for the industry. The specifications of the Hytrex filters can be found in Appendix A.

An additional comparison was attempted against three Porex backwashable depth cartridge filers (labeled as P1, P2, and P3 throughout testing). However, end caps were not available, which prevented reliable observation.

### 2.1.2 Test Filters

All backwashable test filters that were provided for this study had been sintered using polyethylene powder and tested for pore size rating using mercury bubble testing. The specifications of each filter are shown in Table 2.1.

Table 2.1 Test Filter Specifications

| | Design | | Name | Wall thickness T, [cm] | R [cm] | r [cm] | L [cm] | Avg. pore size [µm] |
|---|---|---|---|---|---|---|---|---|
| **Prototype Filters** | Cylindrical depth filter |  | A0 | 1.7 | 3.3 | 1.6 | 25.4 | 25 |
| | | | B0 | | | | | 20 |
| | | | C0 | | | | | 15 |
| | Cylindrical depth filter |  | A1 | 1.1 | 2.75 | 1.6 | 25.4 | 25 |
| | | | B1 | | | | | 20 |
| | | | C1 | | | | | 15 |
| | Cylindrical depth filter |  | A2 | 0.5 | 2.1 | 1.6 | 25.4 | 25 |
| | | | B2 | | | | | 20 |
| | | | C2 | | | | | 15 |
| | Stepped porosity filter |  | G | ~ 0.5 - 0.6 | 3.3 | 1.6 | 25.4 | 15-25 |
| **2nd Generation Prototype Filters** | Cylindrical depth filter |  | D1-I, D1-II | 1.1 | 2.75 | 1.6 | 25.4 | 52 |
| | | | E1-I | | | | | 55 |
| | Cylindrical depth filter |  | F1-30%I, 50%I F1-30%II, 50%II | 1.1 | 2.75 | 1.6 | 25.4 | NA |

The information in Table 2.1 along with all other physical attributes, were provided upon receiving the test filters. Filters names were based first on pore size (represented by the first letter) then by wall thickness (represented by the number following the letter) and finally by triplicate number (three identical filters of each letter number combination). The exception to this naming is with the G, D, E and F1 filters. The G filter has a stepped porosity where the wall thickness is composed of three layers of material;the layer beginning at the inner radius has a pore size of 15 µm, the middle layer increases to 20 µm, and the outer layer is 25µm. The D and E filters are identical in shape but each is made of a different material. The F filters are the same material as the D filter but have different weight contents of fiberglass (indicated by the percentage). Table 2.1 summarizes the test filter attributes and nomenclature. Table 2.2 shows the grouping of filters for each experiment.

Table 2.2 Filter Experiment Grouping

| | | Position | | | | | Description |
|---|---|---|---|---|---|---|---|
| | | Control Filter Skid | | Test Filter Skid | | | |
| | | 1 | 2 | 3 | 4 | 5 | |
| Experiment # | 1 | 5 µm GE | 20 µm GE | A0-1 | B0-1 | C0-1 | Effect of pore size |
| | 2 | 5 µm GE | 20 µm GE | A0-2 | A1-1 | A2-1 | Effect of wall thickness |
| | 3 | 5 µm GE | 20 µm GE | A0-3 | P3/P1 | G-1 | Effect of Shape |
| | 4 | 5 µm GE | 20 µm GE | C2-2 | B0-3 | P2 | Random combinations of Test Filters & Evaluate *Backwashability* of Control Filters |
| | 5 | 5 µm GE | 20 µm GE | G-3 | C0-2 | B0-2 | |
| | 6 | 5 µm GE | 20 µm GE | A2-3, C2-3 | A1-2 | C1-2 | |
| | 7 | 5 µm GE | 20 µm GE | B2-1 | B1-3 | C2-1 | |
| | 8 | 5 µm GE | 20 µm GE | G-2 | C0-3 | D1-I | |
| | 9 | 5 µm GE | 20 µm GE | B1-1 | C1-1 | A2-2, A1-3 | |
| | 10 | 5 µm GE | 20 µm GE | B1-2 | E1-I | D1-II | |
| | 11 | 5 µm GE | 20 µm GE | B2-3 | B2-2 | C1-3 | |
| | 12 | (blank) | | F1-30%I | (blank) | F1-50%I | |
| | 13 | 5 µm GE | 20 µm GE | F1-30%II | (blank) | F1-50%II | |

Notes: Porex Filters: P1, P2, P3 Run 10: Backwashed GE 5 & 20µm Filters Run 12: Pump on Control Skid Failed

## 2.2 Test Procedures

Testing was performed in three ways:

1. Clean membrane specific flux Test
2. Silica Slurry Test
3. Backwash Test

The clean membrane specific flux tests used KBH finished water (mixture of RO permeate and blend water) to determine the clean filter flow. The silica slurry test used a mixture of KBH finished water and silica test dust (silica slurry) to determine filter efficiency. The backwash test used KBH finished water to backwash the cartridge filters to determine repeatability. The three methods are discussed in detail in Sections 2.2.1 to 2.2.3.

### 2.2.1 Clean Membrane Specific Flux Test

To perform the particle free (no silica added) test on the cartridge filters on the test skid, valves were adjusted so flow from the 250 gallon tank could enter the manifold. The pump was turned on, and the manifold feed pressure was adjusted to 45 psi. Gate valves located at the inlet of each cartridge filter

housing on positions 3, 4, and 5 were adjusted until the rotameters at the outlet of each filter indicated 3 gpm (or fully opened). Once all rotameters were stabilized and the manifold feed pressure was stable at 45 psi, flow and pressure readings were recorded. After all readings were recorded, the pump was turned off and the valves were changed to the normal operation configuration. Figure 2.3 shows the flow diagram and valve operations used during the particle free test.

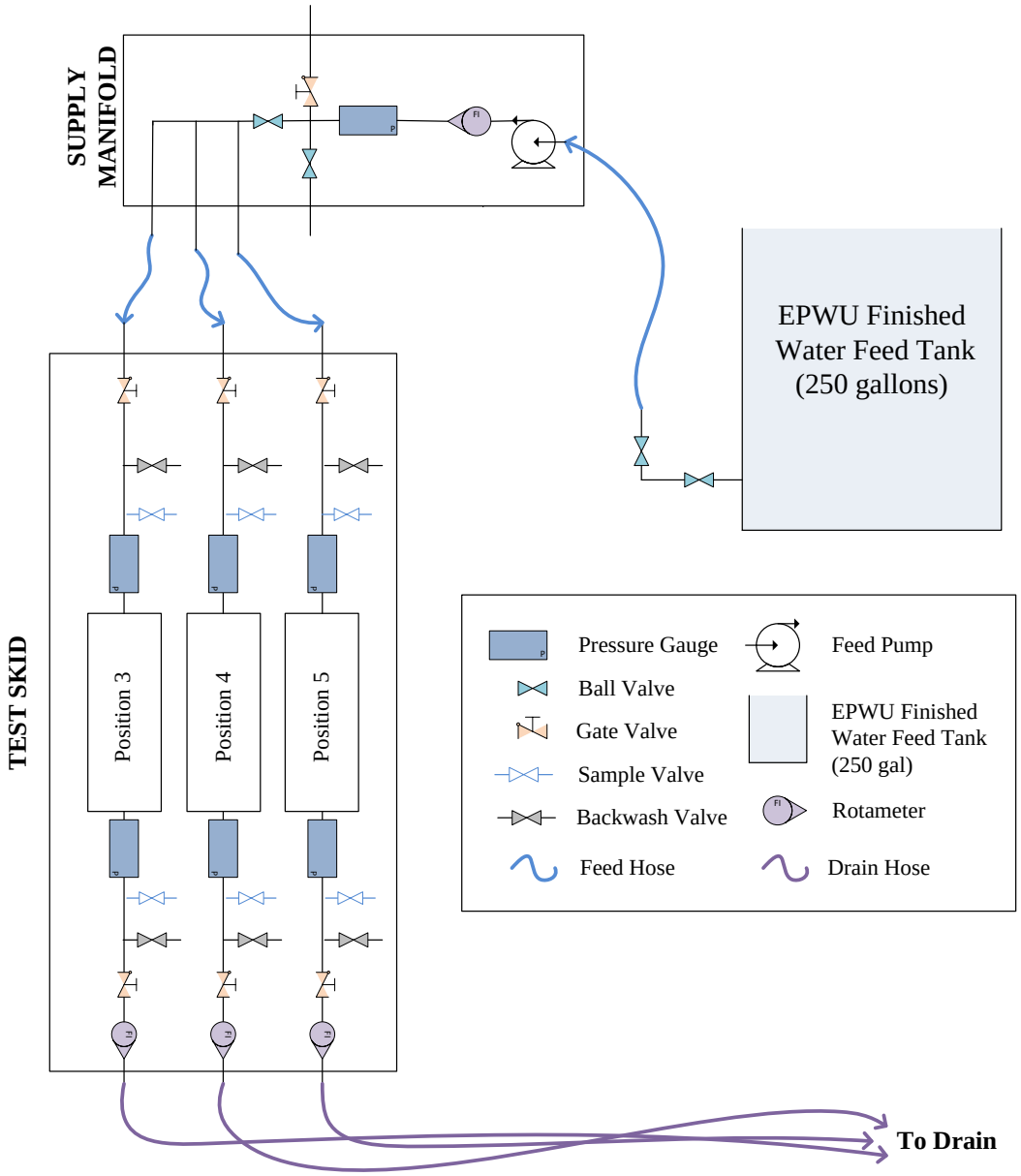


Figure 2.3 Clean Membrane Specific Flux Test - Flow Diagram

### 2.2.2 Silica Slurry Test

To run the silica slurry test, valves were adjusted to allow the flow from the 1500 gallon tank to enter the manifolds on both skids. When set-up was complete, the pumps on both skids were turned on simultaneously along with starting two stopwatches. At least two operators were necessary in order to adjust the manifold pressure and flow rates on each skid during experimental runs.

The manifold pressure was adjusted to 12 psi for the control skid and the flow rate through the cartridge filters installed in positions 1 and 2 was adjusted to 3 gpm. The manifold pressure was adjusted to 45 psi for the test skid and the flow rate through the cartridge filters installed in positions 3, 4 and 5 was adjusted to 3 gpm (or fully opened). Once the flow rate and pressure were stabilized, the first set of data was recorded. Pressure drop, flow rate through filter, and manifold flow and pressure were regularly recorded (typically about every two to four minutes). During each experiment, the manifold pressure was held constant at 12 psi for the control skid and 45 psi for the test skid. The flow rate through each filter would begin to decrease as they began to clog. When this occurred, the operator would adjust the flow rate back to 3 gpm by opening the gate valve ahead of the filter housing inlet. This was a repetitive process as the filter gradually became more and more clogged. Eventually, the gate valve would be completely opened and the flow rate would continue to decrease below 3 gpm. This point was recorded for each filter. The test would run until the flow rate through the filter fell below 0.5 gpm (chosen because it was the lowest marking on the rotameter).

A sample was taken at the inlet and outlet of each filter (for PSD analysis) at the beginning of each experiment soon after the systems reached a steady flow rate of 3 gpm at 45 psi (test skid) or 12 psi (control skid) feed pressure. This was typically performed within the first five minutes of operation. Before obtaining a sample of feed and filtrate water, the sample valve was opened and a stream of the sample water was allowed to flow into a bucket. This ensured a representative sample was obtained. Each sample container was rinsed out three times with the sample water, then filled and sealed.

A similar procedure was followed for turbidity sampling. Vials specifically made for the turbidimeter were used to collect samples at intervals of about 5-10 minutes during the run. Samples were obtained after allowing the sample to flow and triple rinsing the vials first with filtrate, then with

the sample water. Triple rinsing of the vials was necessary to assure removal of excess silica from the previous sampling event. Turbidity samples were taken as long as filters had a flow rate above 0.5 gpm.

After performing each test the feed tank was drained of most of the remaining "dirty" water. About 1-2 inches of water would remain due to the inability to pump all the way to the bottom without causing the pumps to cavitate. The tank was refilled about one third of the way with clean EPWU tap water, and the sump pump was turned on to mix and dilute the remaining silica solution. While mixing, as much as possible of the mixture was pumped out. The sides of the tank were also hosed down to remove any remaining silica. This was repeated several times until a visual inspection indicated most of the silica was removed. If a test was scheduled for the following day, the tank would be refilled. If there was going to be more than two days between tests, the tank would remain empty and was filled at the beginning of the day of the next test. It was necessary to flush water through the hose before filling up either feed tank if a week or more had passed between experiments (typically 30-60 minutes until the water ran clear). This is due to stagnation of water at the CHIWAWA lab at the KBH plant. Additionally, other researchers used the same supply hose for both tap water and RO concentrate. RO concentrate contains substantially higher levels of dissolved constituents and if not properly flushed after use can lead to increased particles from dried salts. Inadequate flushing may be the cause of some inconsistencies between the EPWU tap water samples taken each day as well as the feedwater turbidity. The EPWU tap water was sampled each time to understand the "dirtiness" of the water with respect to particles.

### 2.2.3 Backwash Test

The test skid is used for backwashing. After testing, the prototype filters on this skid are backwashed by reversing flow through the cartridge for 90-120 seconds or until the housing is visibly clear with a flow between 3 and 10 gpm.

All re-useable filters were backwashed individually after testing. Figure 2.4 shows how the EPWU tap water from the 250 gallon tank was used to backwash the filters by simply adjusting valves to allow reverse flow through the test skid. Filters were backwashed for 90-120 seconds (or until the backwash effluent was clear) at a manifold pressure between 20 and 30 psi and/or a flow between 4 and

10 gpm. Manifold flow and pressure, along with the pressure drop across the filter and outlet filter flow rate were recorded for each backwash. Some of the earlier experiments did not include backwash flow rate data, because rotameters were not yet installed. The GE Hytrex 5 and 20 µm filters were also tested for "*backwashability*."

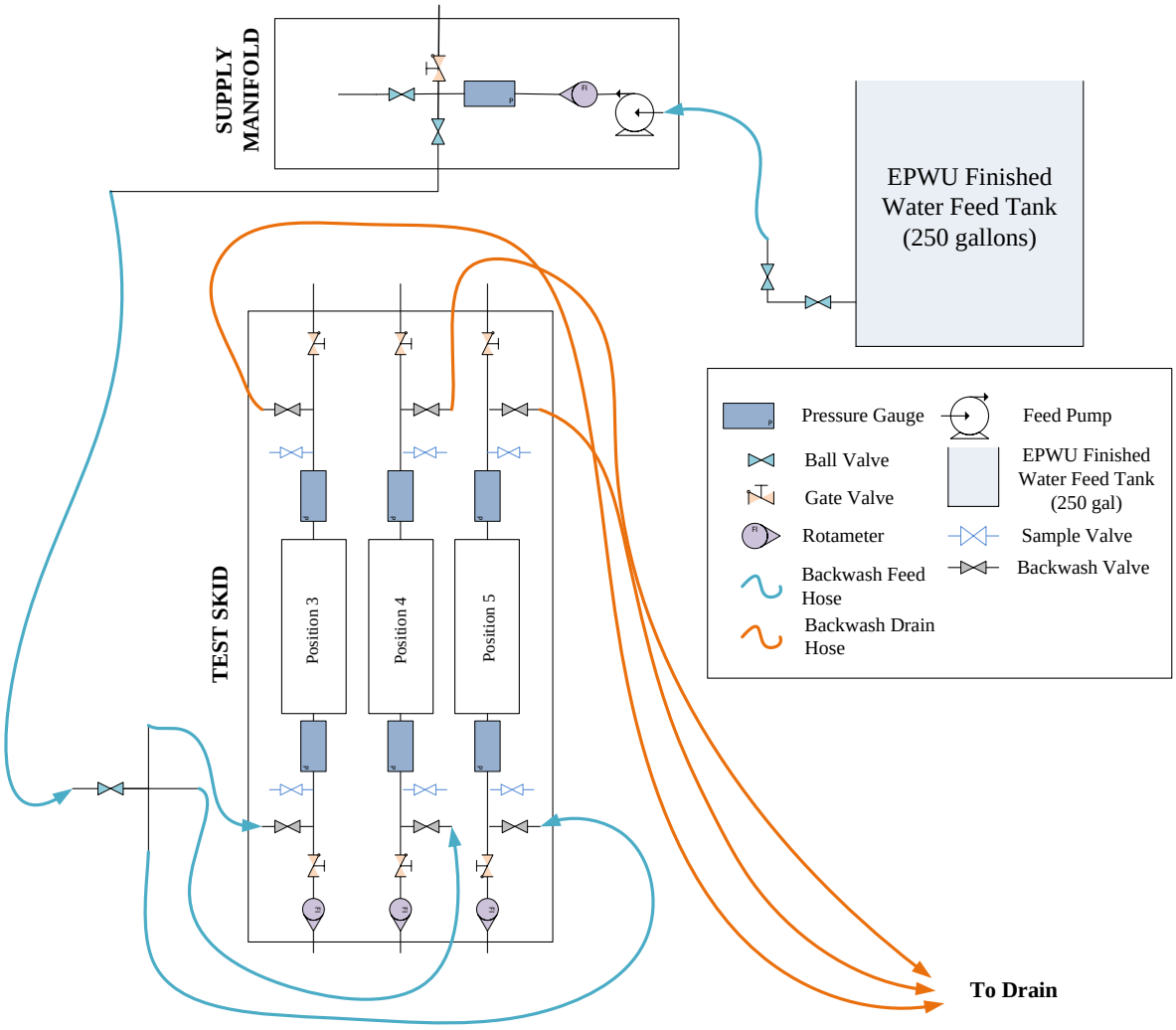


Figure 2.4 Backwash Flow Diagram

## 2.3 Experimental Controls and Monitoring

Methods for testing cartridge filters vary from one application/industry to the next and result in inconsistencies when attempting to compare performance. It is necessary to specify conditions under which the manufacturer's operating parameters for a cartridge filter were generated; the liquid being filtered, the required pressure, the desired particle reduction, etc. In order to assure the validity and comparability of the laboratory scale test several controls were established.

### 2.3.1 Flow

On the supply manifold, a Goulds G&L Model LB Series Booster Pump was used to direct/pump clean water and silica slurry to the test skid. A second pump (same model; 1hp) was used to pump only silica slurry to the control test skid. A Blue-White Industries, Ltd. Polysulfone Molded F-461 Rotameter was located at the outlet of each pump to monitor flow through both manifolds. The F-461 Rotameters were rated for flow from 0.5 to 5.0 gpm.

A 1 inch threaded brass gate valve was used to control the flow through each individual filter. This flow rate was monitored on Blue-White Industries, Ltd. Polysulfone Molded F-460 Rotameters located at the outlet of each filter's housing. The F-460 Rotameter was rated for flow from 0.5 to 5.0 gpm. At the beginning of each test the gate valves were adjusted until the exit flow read 3 gpm. The flow through each cartridge filter was monitored and recorded at regular time intervals.

### 2.3.2 Pressure

A gate valve located on the recirculation line on each manifold was used to control the manifold feed pressure for each skid. Granger Filled, 1 ½ inch, 60 psi, Pressure Gauges (Model# 4FKY1) were used to monitor the pressure. Feed pressure to the test skid was maintained at 45 psi, while the control skid operated at 12 psi. The manifold pressure was monitored and recorded at regular time intervals.

The same pressure gauges were used on both the control and test skid. They were placed at the inlet and outlet of each cartridge filter housing. The pressure difference between the two gauges was monitored and recorded at regular time intervals to determine the pressure drop across each filter during testing.

### 2.3.3 Flux

Membrane flux was calculated for each test filter, because the filter performance appeared to resemble the performance to MF and UF membranes. In *Water Treatment Principles and Design* (MWH, 2012, p. 852), membrane flux, *J*, is defined as:

$$J = \frac{Q}{a} = \frac{\Delta P}{\mu \kappa_m}$$

Where $J$ = volumetric water flux through membrane, L/m$^2$·h or m/s

$Q$ = flow rate, L/h

$a$ = membrane area, m$^2$

$\Delta P$ = differential pressure across membrane, bar

$\mu$ = dynamic viscosity of water, kg/m·s

$\kappa_m$ = membrane resistance coefficient, m$^{-1}$

In addition to membrane flux, the specific flux (MWH, 2012, p. 853) was also calculated for each membrane. In this research, the flux at standard temperature, $J_s$, was assumed to be equal to the flux measured at room temperature, $J_m$ (MWH, 2012, p. 853). The membrane flux, *J*, was substituted for $J_s$ in the specific flux, $J_{sp}$, calculation (MWH, 2012, p. 854):

$$J_{sp} = \frac{J_s}{\Delta P}$$

Where $J_s$ = flux at standard temperature, L/m$^2$·h·bar

Results of the flux analyses for all filters are discussed in Section 3.2.1.

### 2.3.4 Cartridge Filter Fouling Index

Although the MFI [m$^{-1}$] is used mainly for membrane filtration (MF, UF and NF), an initial attempt was made to characterize the fouling of the cartridge filters in this study. However, fundamentally, the MFI assumes a flux behavior that is proportional to the reciprocal of specific throughput, which was inconsistent with the fouling trends observed in this research.

The new index was derived based on an exponential decay as a function of specific throughput, as shown in of Figure 2.5. The Cartridge Filtration Fouling Index or *CFFI* [m$^{-1}$] is defined as:

$$CFFI = slope\ of\ \left[-ln\left(\frac{J_{sp}}{J_{sp_0}}\right)\right]\ versus\ [V_{sp}]\ \forall\ V_{sp} > 0$$

Where $J_{sp_0}$ = clean water specific flux, L/m2·h·bar

$V_{sp}$ = Specific Throughput, L/m$^2$

Like the MFI, a larger *CFFI* indicates a faster rate of fouling (steeper slope), as shown in Figure 2.6 (That is, the *CFFI* value is the slope of the linearized form, which is equal to the exponential coefficient of normalized specific flux.) The *CFFI* was used to compare the performance of the cartridge filters in this study. Results of the analysis are discussed in Section 3.2.3.

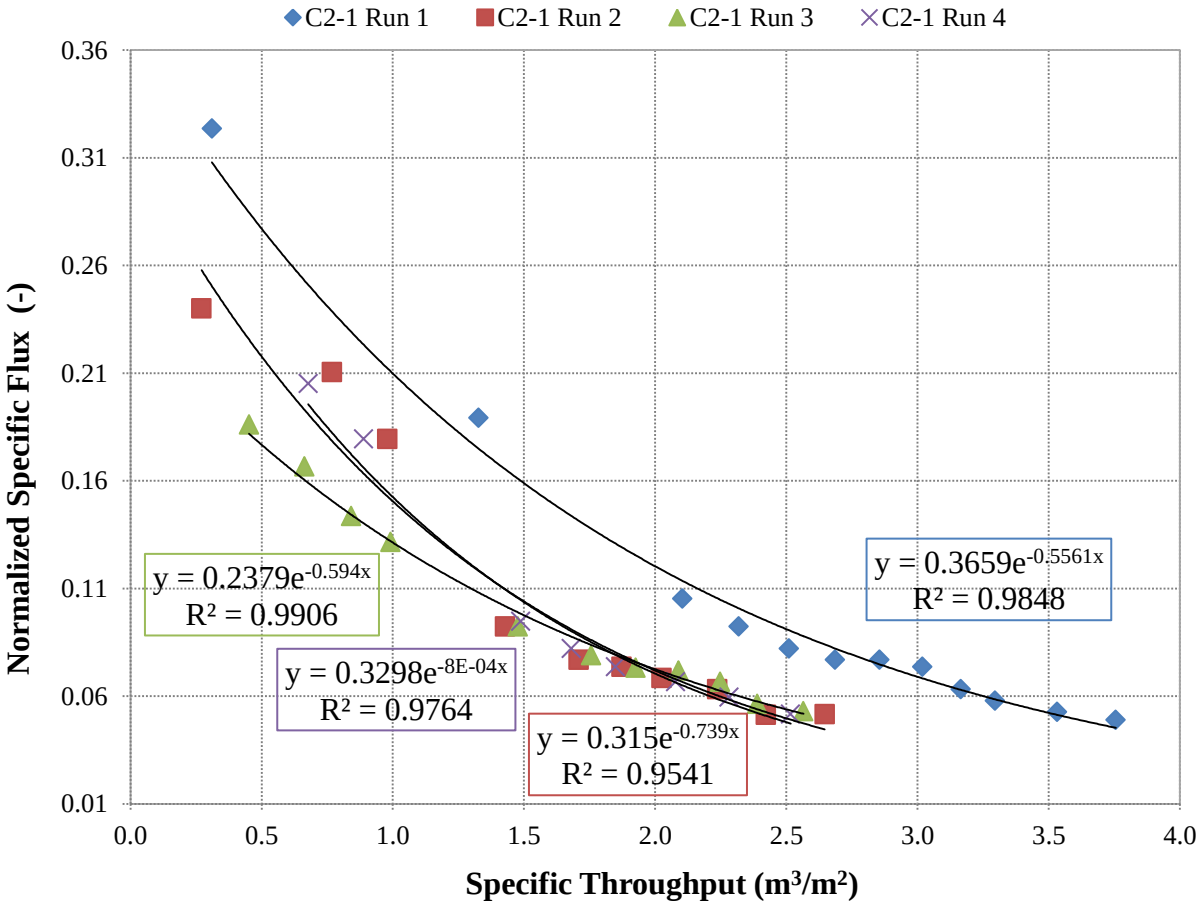


Figure 2.5 Normalized Flux vs. Specific Throughput

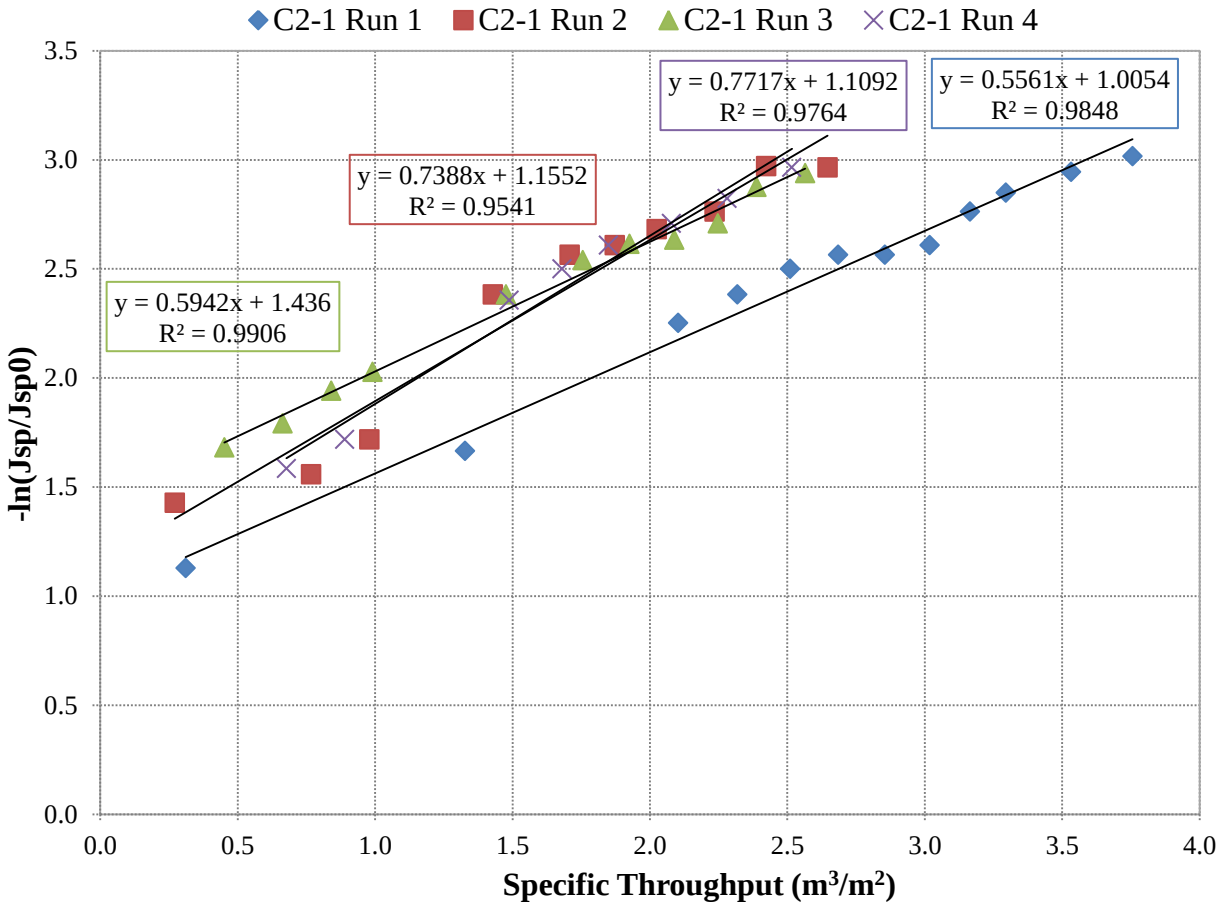


Figure 2.6 $-\ln(J_{sp}/J_{sp0})$ vs. Specific Throughput

### 2.3.5 Backwash

The test skid was capable of evaluating backwashing. After testing, the filters on this skid were backwashed by reversing flow through the cartridge by reversing ball valve positions. The backwash time was monitored with a stopwatch and by manually starting and stopping flow by turning the pump on and off. The flow rate was monitored using rotameters located at the outlet of the backwash flow lines. The backwash was terminated based on visual inspection of the clarity of water in the cartridge filter housing.

### 2.3.6 Slurry Composition

Figure 2.7 summarizes the particle size distributions for ACCTD and ACFTD (discussed in Section 1.1.1). Since the ACCTD and ACFTD are no longer manufactured, several alternatives were sought for use in this study.

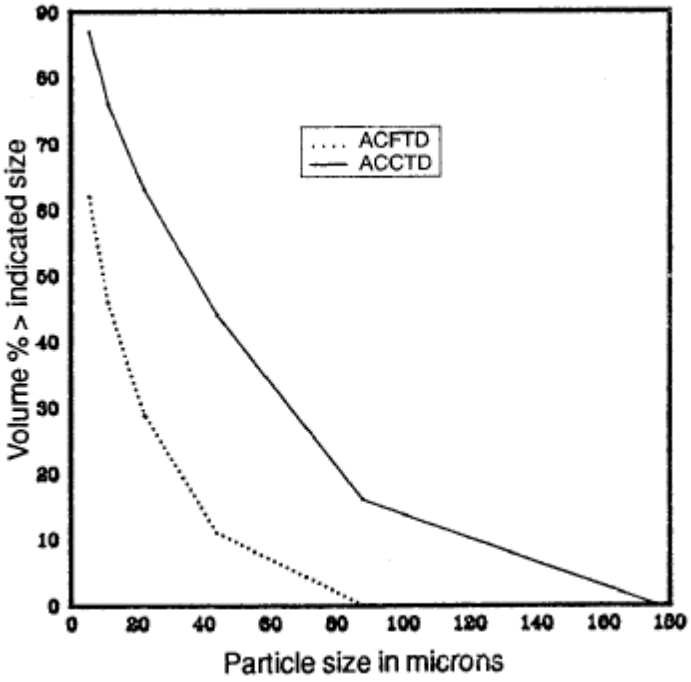


Figure 2.7 Particle Size Distribution of ACCTD and ACFTD
*Source: (Williams, Testing the Performance of Spool-Wound Cartridge Filters, 1992)

The National Institute of Standards and Technology (NIST) has products similar to ACCTD and ACFTD that are available for purchase - Reference Material 8631a (Medium Test Dust) and Reference Material 8632 (Ultrafine Test Dust). The Medium Test Dust was the first alternative tested. It had the desired particle size distribution (PSD), as shown in Figure 2.8, which would allow the particles to remain suspended in the tank for the duration of the test. However, it was costly, and a large amount would be needed to test all the filters.

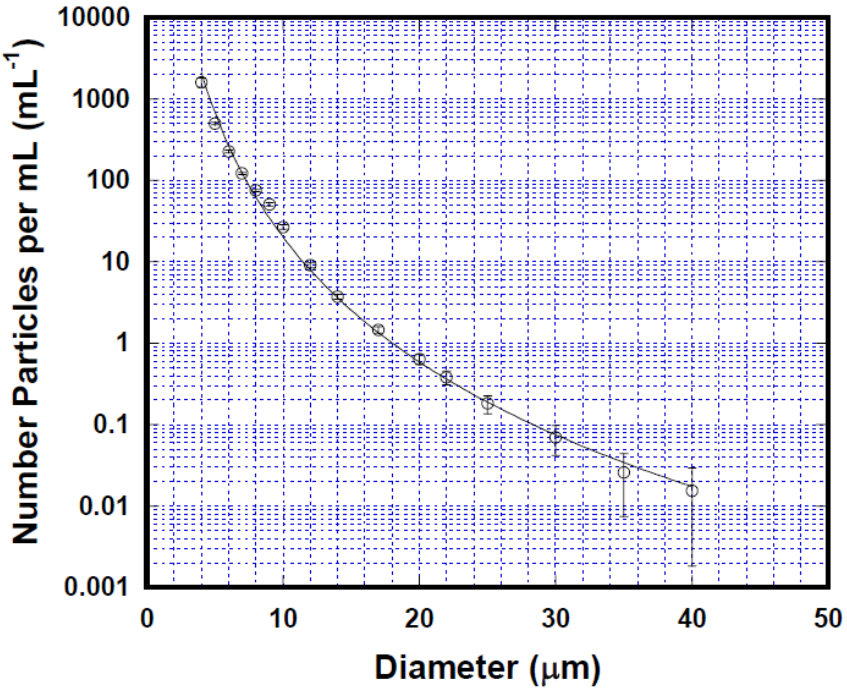


Figure 2.8 NIST Reference Material 8631a (Medium Test Dust) Particle Size Distribution
*Source: (NIST, 2011a)

A second attempt was made using "play sand" because of its affordability. However, the PSD range was much wider than the NIST dust. The majority of the particles could not pass through the filter and instead formed a sand filter around the cartridge.

The last attempt, also a lower cost option, used a fine ground silica powder called SIL-CO-SIL 106 (SCS 106) from the U.S. Silica Company; Ottawa, IL Operations (US Silica, 2013). Figure 2.9 shows the PSD of SCS 106 and Appendix B includes an information sheet for the product. The SCS 106 had a slightly wider PSD range compared to the NIST test dust, and some of the larger particles did settle faster to the bottom of the feed tank, but most remained suspended for the duration of the test. Preliminary trials with the SCS 106 indicated that it was the best option.

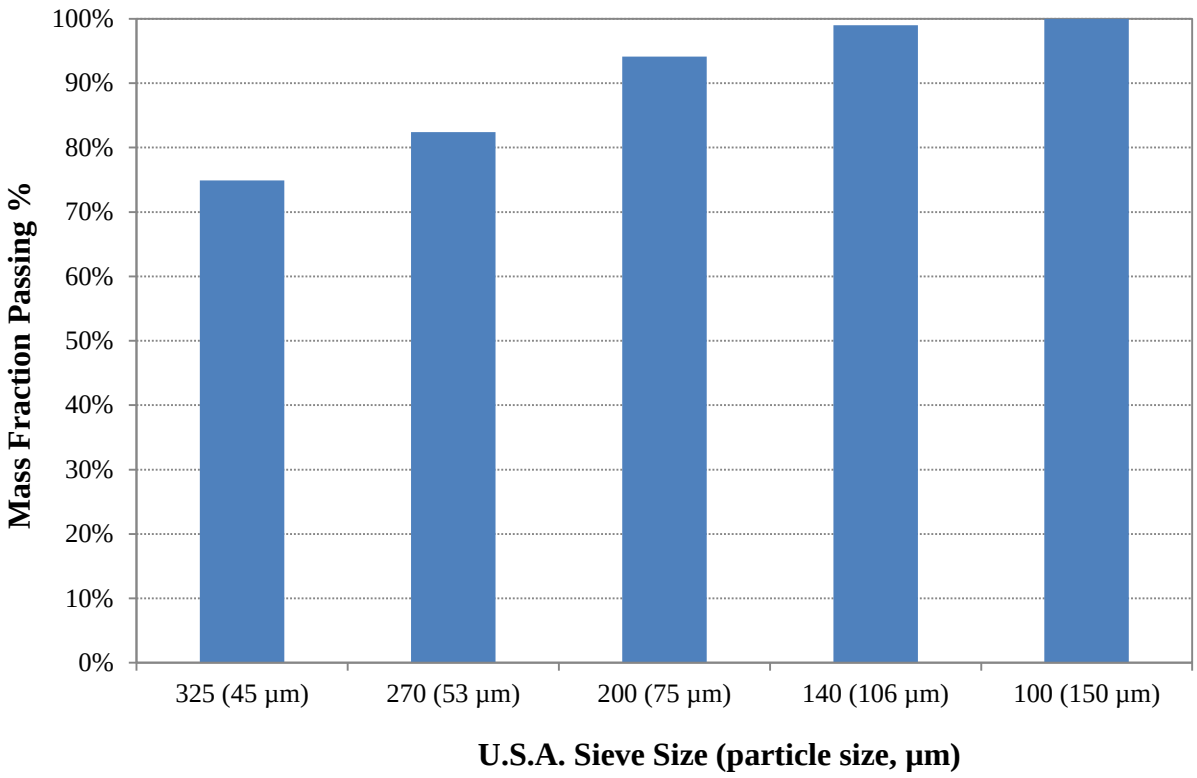


Figure 2.9 Sil-CO-Sil 106 Particle Size Distribution
*Adapted from: (US Silica, 2013)

To create the silica slurry, SCS 106 was mixed with KBH's finished water. The approximate concentration of SCS 106 necessary to foul the filters was determined by several preliminary tests conducted using the control filters. Testing showed that a concentration of 0.44 g/L of SCS 106 would be sufficient to simulate "dirty" water with a measured turbidity between 50 to 70 NTU and clog the filters within one to two hours. Seawater is reported to have a turbidity of 2-50 NTU during the storm season (Desormeaux, 2009), so this turbidity range is slightly higher and represents a form of challenge test. The maximum run time (based on flow and volume of silica slurry prepared) was estimated to be one to two hours.

To prepare the silica slurry, the 1500 gallon capacity feed tank was filled with approximately 1300 gallons of KBH finished water and the sump pump was activated to allow the water in the tank to begin a mixing motion. The SCS 106 powder was weighed and carefully added to the opening at the top of the tank. After the silica and water were sufficiently mixed, the turbidity was measured for samples of slurry collected from the top and bottom of the tank to check for uniformity of the mixture. The samples

were poured into clean turbidity sample vials and tested on a Hach 2100P turbidimeter. Care was taken when collecting samples to keep vials clean from particles and avoid bubble formation, which can alter readings and invalidate the analysis. If sample readings were within the desired turbidity range between 50 and 70 NTU, then the silica slurry was considered ready for use. The slurry was used to feed both skids.

The 1500 gallon tank was rinsed several times after testing, but it was not possible to remove all of the silica particles. The 0.44 g/L concentration of Sil-Co-Sil 106 seemed to allow some particles to settle during the experimental runs, which resulted in leftover silica at the bottom of the tank and increasing turbidity throughout experimental runs. The Sil-Co-Sil 106 concentration was reduced to 0.32 g/L in later runs in order to maintain the turbidity between 50 and 70 NTU.

### 2.3.7 Field Analysis (Turbidity)

All turbidity samples were collected and analyzed at the test site. Samples were collected at the feed and filtrate of each cartridge filter several times throughout testing. Samples were then analyzed using a Hach 2100P turbidimeter.

### 2.3.8 Particle Size Distribution (PSD) and Particle Counter

A particle counter (also called a Coulter Counter) counts the number and sizes of particles within a given volume of liquid/sample. Samples for PSD analysis were collected in new containers which were triple-rinsed before filling to mitigate contamination. Two samples were collected per filter: feed and filtrate. Samples were transported to the CIDS lab for analysis on the Multisizer 4 Coulter Counter.

**Background**

The Coulter Counter draws in a specific volume of prepared sample through the orifice of an aperture. The CIDS lab has several aperture sizes are available (30-µm, 100-µm, 200-µm, and 400-µm) and are selected based on the desired particle distribution range to be analyzed. Each aperture is rated to detect particles from 2 to 60% of the aperture size. The machine has one electrode inside the aperture and another outside (submerged in the solution). The difference in voltage between the electrodes as particles are drawn through the aperture and the size of the orifice indicates the size of the particle. The

machine also records the number of particles drawn through the orifice within a specific volume. Figure 2.10 shows Coulter Counter electrode, aperture, and sample placement.

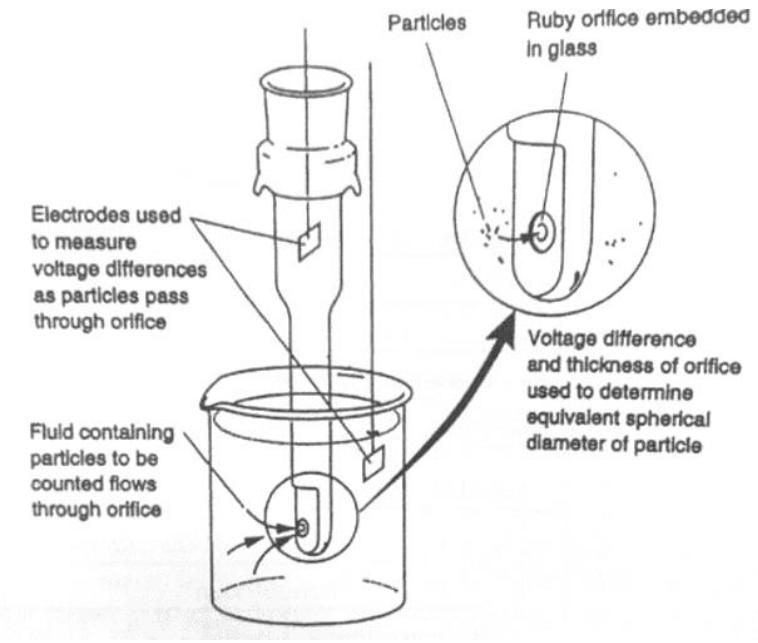


Figure 2.10 MS4 Electrode and Sample Vial Diagram
*Source: (MWH, 2012, p. 36)

The Coulter Counter requires samples to be added to an electrolyte solution (the sample solution must have enough electrolyte to allow conductivity in the solution). Each sample was therefore diluted (ratio of sample to electrolyte not to exceed 1:1) before analysis by the Coulter Counter. The electrolyte used for the analyses is called Isoton II diluent (a low-particle sodium chloride solution). Running an analysis is an iterative process dependent on particle concentration and size distribution.

**Instrumentation**

The Beckman MS4 Coulter Counter (MS4), shown in Figure 2.11, was used to analyze the particle size distribution of the feed and filtrate water samples for each cartridge filter tested. A user friendly panel on the front allows for quick adjustments of the stir bar during a sample analysis. There is a separate area inside the machine which contains two glass jars; one for holding new electrolyte and the other for waste. MS4 analyses were able to provide data for the calculation of the removal efficiency for each filter.


Figure 2.11 Beckman Multisizer 4 Particle Analyzer at UTEP

**Instrument Calibration**

The MS4 uses standardized beads to calibrate particle size measurements. A calibration check was performed each day that samples were analyzed by following the "Calibrate Aperture Tube Wizard" on the provided MS4 software. This involved adding a set amount of calibration beads to a clean Accuvette (container designed specifically for MS4 use) filled with Isoton II diluent. A full calibration was performed on the MS4 each time a new container of Isoton II diluent was opened.

A full calibration was performed by running the "Change Aperture Tube Wizard" and then running four additional analyses using four sizes of calibration beads. To fully calibrate the 100 µm aperture, an Accuvette was filled with 20 mL of Isoton II diluent. This Accuvette was analyzed as a blank and used as a "noise level" indicator. The Isoton II blank was considered acceptable if the noise level was lower than 2 µm and the particle count was lower than 300 for a 2000 µL sample. After analysis, the Accuvette was refilled with Isoton II diluent up to the 20 mL line. One drop from a "thoroughly shaken" bottle of 2 µm standardized beads was added to the blank and analyzed as the first calibration point. It was critical to "thoroughly shake" the calibration bottle in order to mix the beads with the supporting fluid to assure homogeneous concentration of beads with each drop and produce an accurate calibration. The Accuvette was gently swirled to assure proper mixing. It was important not to shake the Accuvette so as to avoid forming bubbles, which alter MS4 readings (detects air bubbles as overly-high particle counts or as a leak). If performed correctly the analysis would show a clear peak

very close to 2 μm. The second calibration point was performed with one drop of the 5 μm calibration beads added to the same Accuvette (i.e. no rinsing or refilling). The mixture was then carefully swirled and analyzed to obtain two peaks at 2 μm and 5 μm. The process was repeated a third time by adding one drop of the 10 μm calibration beads to the same Accuvette, and three peaks were obtained at 2, 5, and 10 μm. The last calibration followed the same procedure using one drop of the 20 μm calibration beads. If all peaks were within range of the specified average particle size for each bottle of calibration beads (e.g. the 10 μm calibration beads have an average particle size of 10.18 μm), then the calibration was declared complete and successful. In some instances more than one drop of calibration beads needed to be added to the Accuvette in order to get a clear prominent peak. This occurred mostly as a result from not thoroughly shaking the calibration bead containers before use. All full calibrations and calibration checks were recorded and used to calculate parameters necessary for sample analysis.

After calibration it was important to clean out the accumulated beads from the inside of the aperture. The outside of the aperture was rinsed with DI water (carefully to avoid water splashing inside the machine) and a fresh Accuvette with new Isoton II diluent was prepared and analyzed as a blank (making sure to check the "flush aperture tube" box before analyzing). Depending on how many calibration particles went through and remained in the system, it was sometimes necessary to repeat the process. As soon as the Isoton II blank analysis showed a sufficiently low particle count (less than 300 for a 2000 μL sample), sample analyses could be performed.

**Sample Preparation**

A 100 μm aperture was selected for this project to show the particle size distribution of each sample between 2 and 38.1 μm. Analyzing a sample is an iterative process, mostly dependent on how concentrated the sample is with respect to particles. Typical dilutions for feed samples ranged between 0.1 to 0.4 mL of sample to 20 mL electrolyte. Filtrate samples ranged between 0.3 to 0.5 mL sample per 20 mL of electrolyte for control filters and anywhere from 1:20 mL (sample:electrolyte) to 5:15 mL for the backwashable filters. Dilutions for the EPWU feedwater ranged between 5:15 mL to 10:10 mL (which is the maximum dilution recommended for Isoton II diluent).

Certain parameters were utilized for each analysis based on sample type. All control filter feed and filtrate samples were analyzed using the volumetric setting (2000 µL) while test filter filtrate samples were analyzed using the time setting (300 seconds). The amount of time (and volume) is determined based on particle count number. For example, the ideal particle count range for the 100 µm aperture is 10,000 to 18,000 particles. An analysis within this range will provide a better ability to visualize the particle size distribution of the sample. As a result, a sample will need to be run longer or shorter in order to achieve a count within the range. For these reasons, the process is iterative since the concentration of particles in the sample is unknown.

Along with the above parameters, several procedures were followed while running samples. Between high count samples the aperture was carefully rinsed with DI water and at least one blank was run to flush the system of particles. Aperture rinsing was performed with a squirt bottle (care was taken to capture the run off in a container to avoid getting the inside of the MS4 wet). Rinsing between high particle count samples minimizes the number of particles left behind from a previous sample. Blanks and rinsing between low count samples was not necessary due to the very low number of particles present.

**Analysis Process**

Raw particle counts were performed with a 100 µm aperture in the MS4, and the raw data were processed using the guidelines described by Nason (2006, pp. 56-57).

### 2.3.9 SEM

After all experiments were performed, the filter manufacturer sectioned several filters and analyzed the surface using a Scanning Electron Microscope (SEM). The results of this analysis are discussed in Section 3.1.3.

# Chapter 3: Results and Discussion

All test and control filter feed and filtrate samples were collected and analyzed by comparing filter efficacy and hydraulic performance.

## 3.1 Filter Efficacy

The efficacy of the test filters was analyzed by observation of trends within test filter types and comparisons to the control filters. Observations were made based on turbidity, particle size distribution, and a TSS estimation based on feed and filtrate samples collected during each experiment for each filter tested. In addition a visual comparison was made using SEM micrographs provided by the filter manufacturer.

### 3.1.1 Turbidity

Figure 3.1 contains average removal efficiencies based on feed and filtrate turbidity readings taken at regular time intervals throughout each experiment (MWH, 2012, p.217). The data show a significant improvement in particle reduction by the prototype filters (A, B, C, and G) in comparison to the control filters (5 μm and 20μm GE Hytrex).

Observing the prototype filters alone, removal efficiency generally increased with decreasing pore size (smaller pore size indicates removal of smaller particles). The second generation prototype filters (D1, E1, and F1 filters) had smaller turbidity reductions compared to the original prototypes. First the lower concentration of fiberglass in the F1-30% I and II filters showed higher turbidity reduction compared to the F1-50% I and II filters. The filters with higher fiber content clearly block fewer particles, possibly due to more gaps and spaces between fibers. There may also be less of a homogeneous matrix with the higher fiber content. Observing the D and E filters, the D filter shows higher turbidity reduction. The E filter showed the closest performance to the GE control filters with a turbidity reduction efficiency of about 50%.

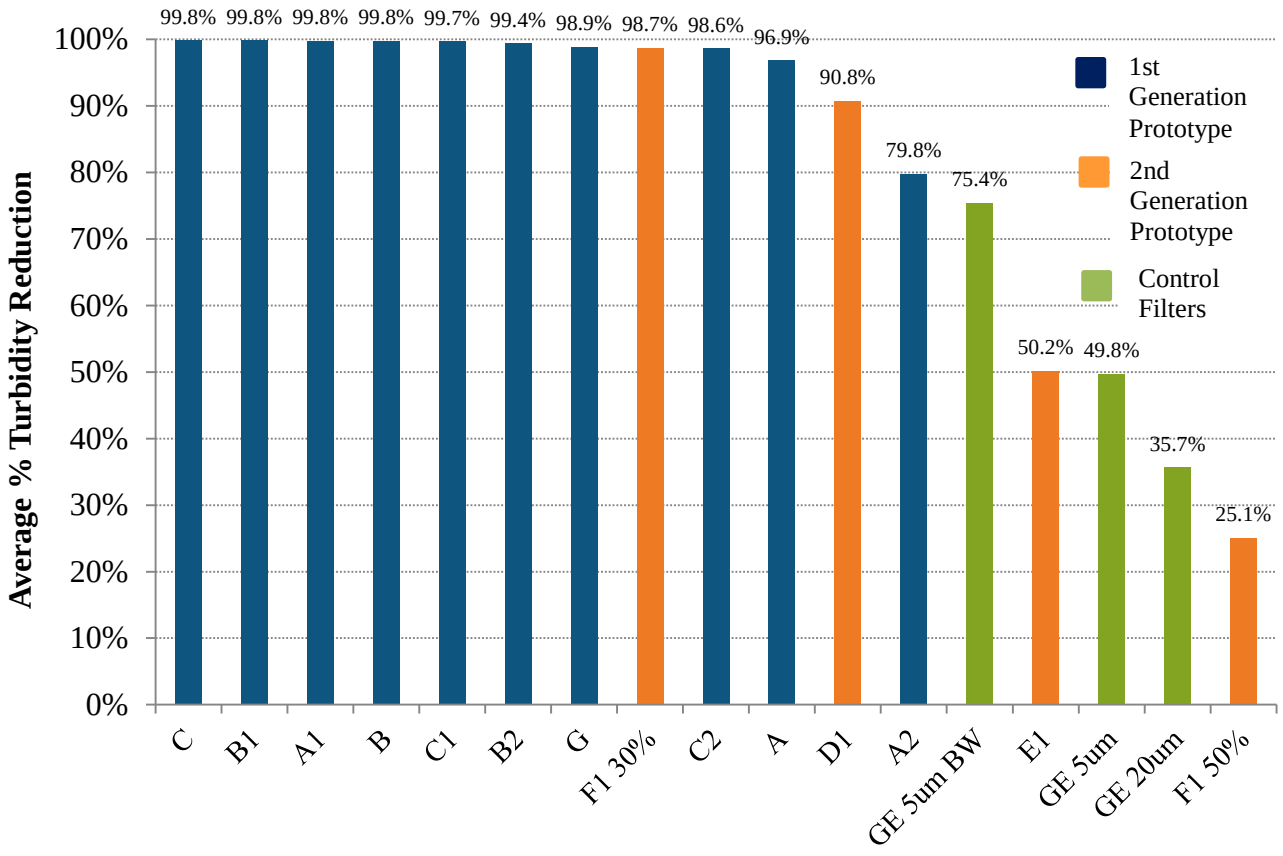


Figure 3.1 Average Turbidity Reduction

The highest level of reduction in turbidity obtained with GE filter elements was about 75% with the 5 µm filter that was backwashed. A possibility for the greater removal could be indicative of inability to be backwashed, leading to accumulation of particles and formation of a cake layer that is improving the actual filter performance over time. Testing of the control filters as single-use showed very low turbidity reductions of about 35% with the 20 µm filters and about 50% with the 5µm filters. Both removal values are low when compared to typical 98 to 99% removals for the majority of the backwashable test filters.

Overall turbidity analyses show improved filtrate water quality of the first generation prototype filters and a closer performance to the control filters with the second generation prototypes.

### 3.1.2 Particle Size Distribution (PSD)

Feed and filtrate particle analyses on the MS4 were used to determine particle removal efficiency for each filter (MWH, 2012, pp.655-656). The data collected included the number of particles, ΔN

[#/mL], along with particle diameter, $d_p$ [µm] (MWH, 2012, p. 38). A plot of ΔN vs. $d_p$ was constructed for each filter and includes the feed, filtrate and particle removal efficiency curves (see Appendix C). In terms of smoothing the raw data, a power function was the best fit for the test filter data (Figure 3.2), while a hyperbolic cosecant function was a better fit for the control filter data (Figure 3.3).

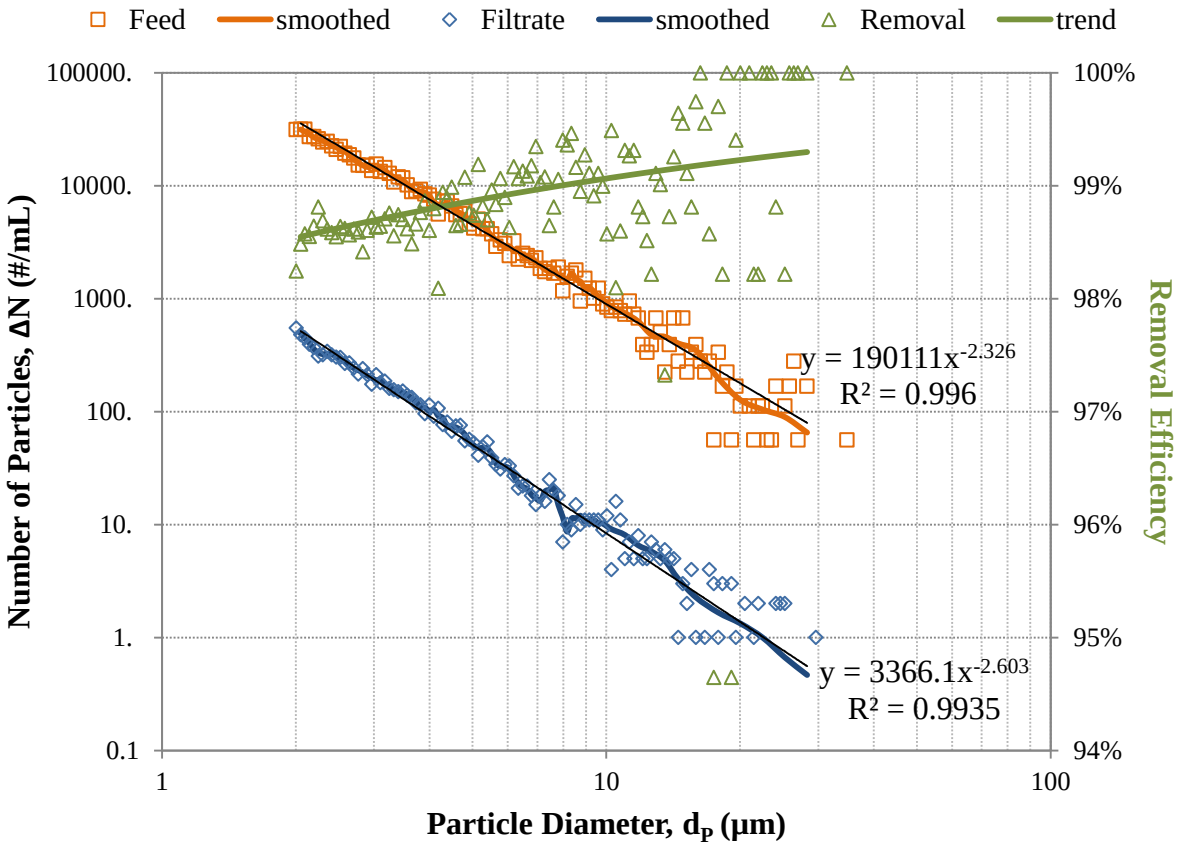


Figure 3.2 Typical Test Filter Removal Curve

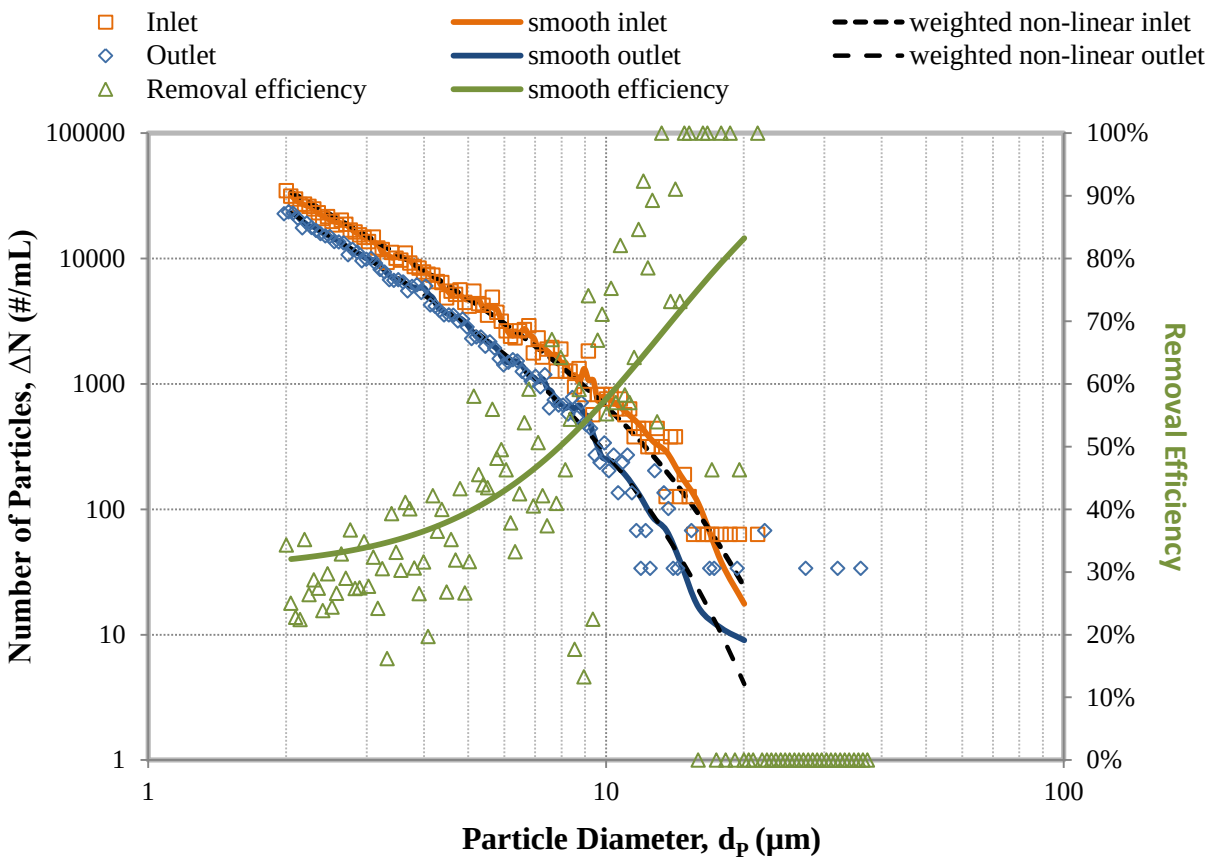


Figure 3.3 Typical Control Filter Removal Curve

Figure 3.4 shows the feed particle concentrations of the A, B, C, D, and G filters for all experiments. Variation is about one order of magnitude. Data in Figure 3.5 for the filtrate particle concentrations of the same filters indicate a difference of about three orders of magnitude. Together these graphs indicate the variance in silica slurry feed concentrations with each experiment as well as difference in particle reduction by the filters.

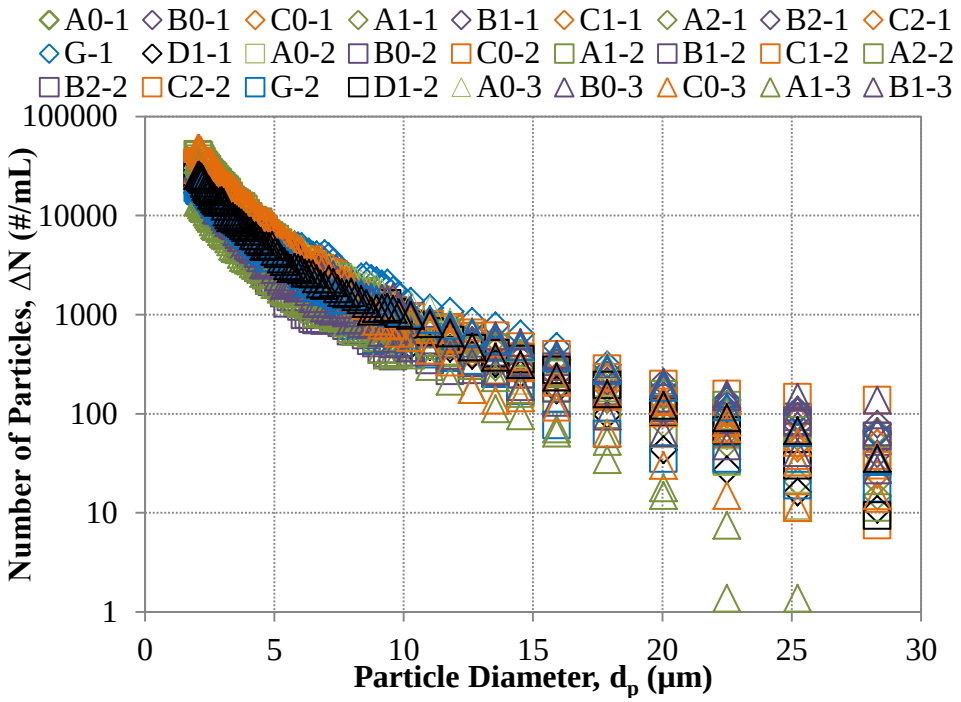


Figure 3.4 Test Filter Feed Concentrations

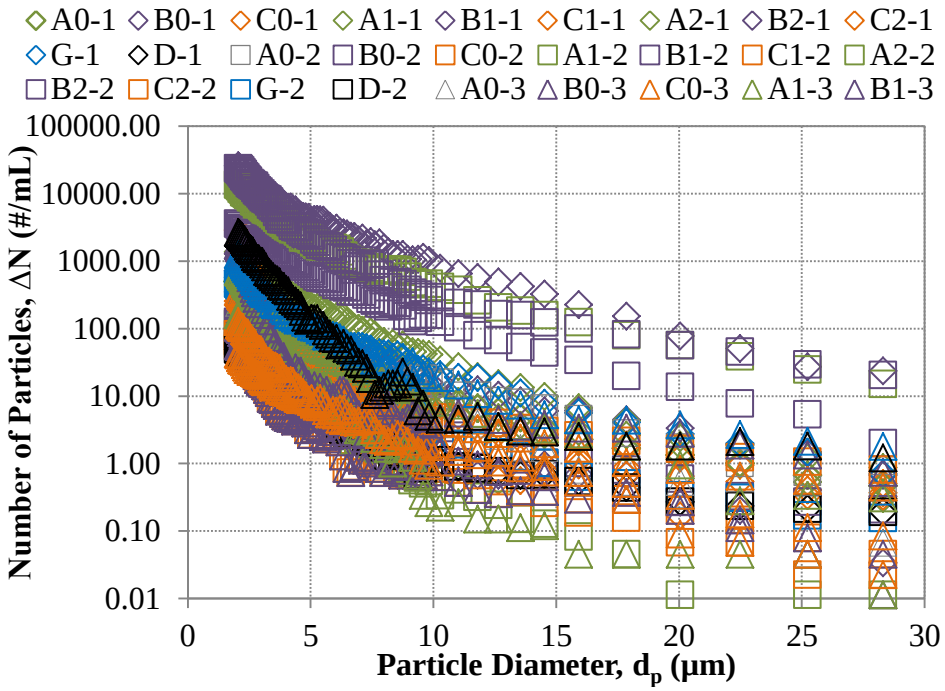


Figure 3.5 Test Filter Filtrate Concentrations

Although there was not a visible trend in wall thickness, there was a visible trend in pore size with respect to particle reduction. Figure 3.6 shows that the range in particle removal efficiency

decreases with increasing pore size. This indicates higher particle reduction with lower pore size. The 25 µm "A" filters vary in particle removal efficiency from 94-99% while the 20 µm B filters show less variation (98-99%) and the 15µm C filters show the smallest variation (above 99%). The step-porosity G filter showed particle removal efficiencies between that of the 15 µm and 25 µm filters (96-99%).

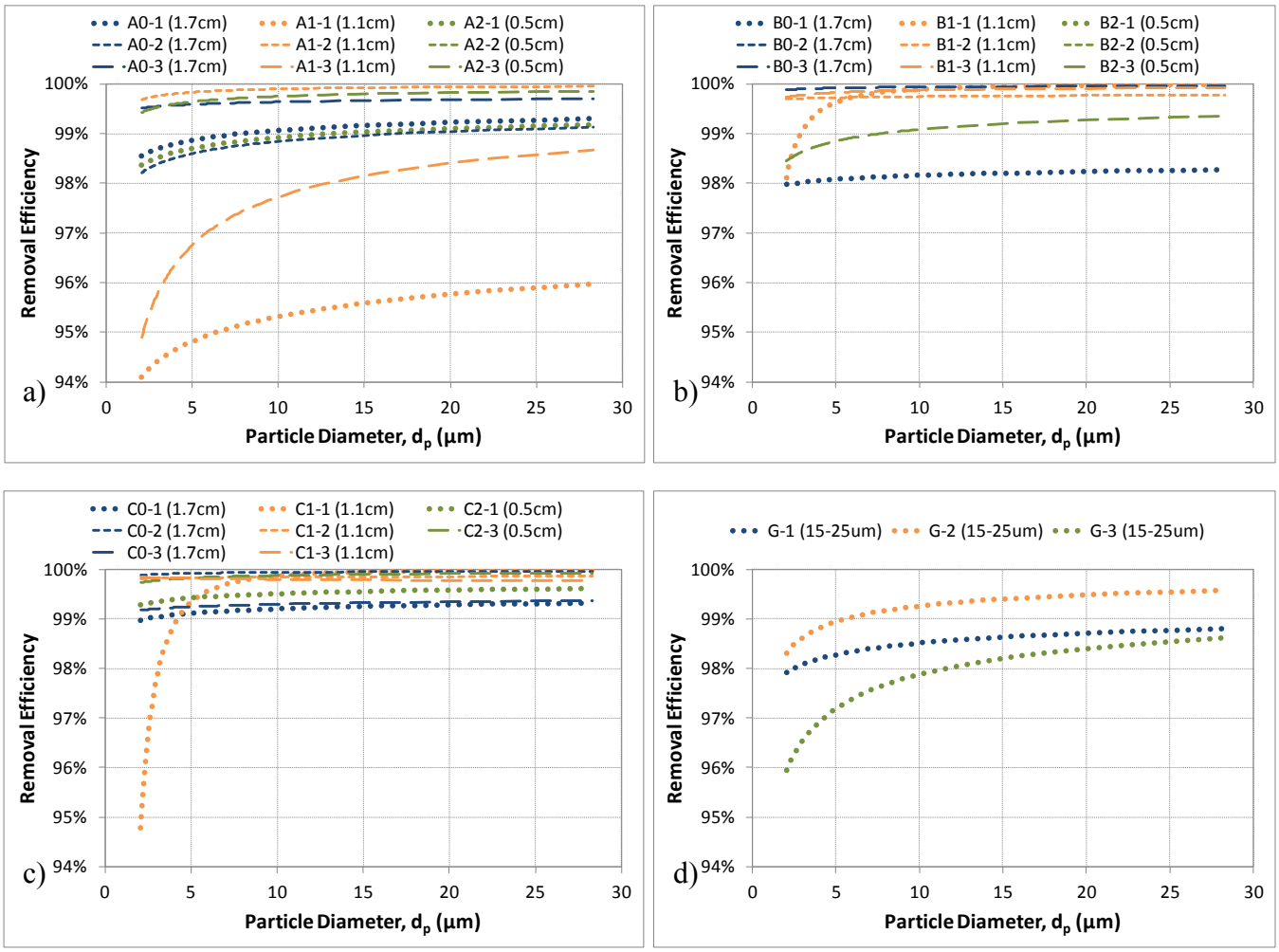


Figure 3.6 Prototype Filter - Particle Removal Efficiency
a) A filters; b) B filters; c) C filters; d) G filters

The particle removal efficiencies of all 5 µm control filters are represented by a box and whisker plot in Figure 3.7. There is a wide variation between the filters indicating a lack of consistent performance. For a particle size of 5 microns, a maximum particle reduction was about 65%.

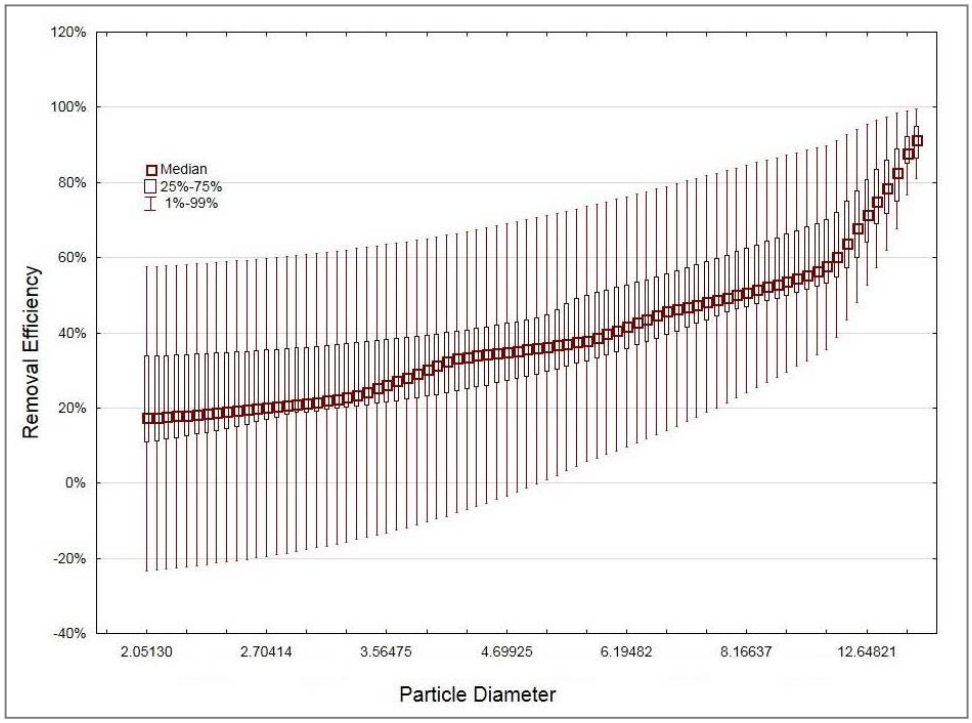


Figure 3.7 Removal Efficiency for 5 μm GE Filters - All Experiments

The particle removal efficiencies of all 20 μm control filters are represented by a box and whisker plot in Figure 3.8. There is, again, a wide variation between the filters indicating a lack of consistent performance. For a particle size of 5 microns, the maximum particle reduction was about 45%. (It is possible that unsteady conditions could result in negative particle removal efficiencies.)

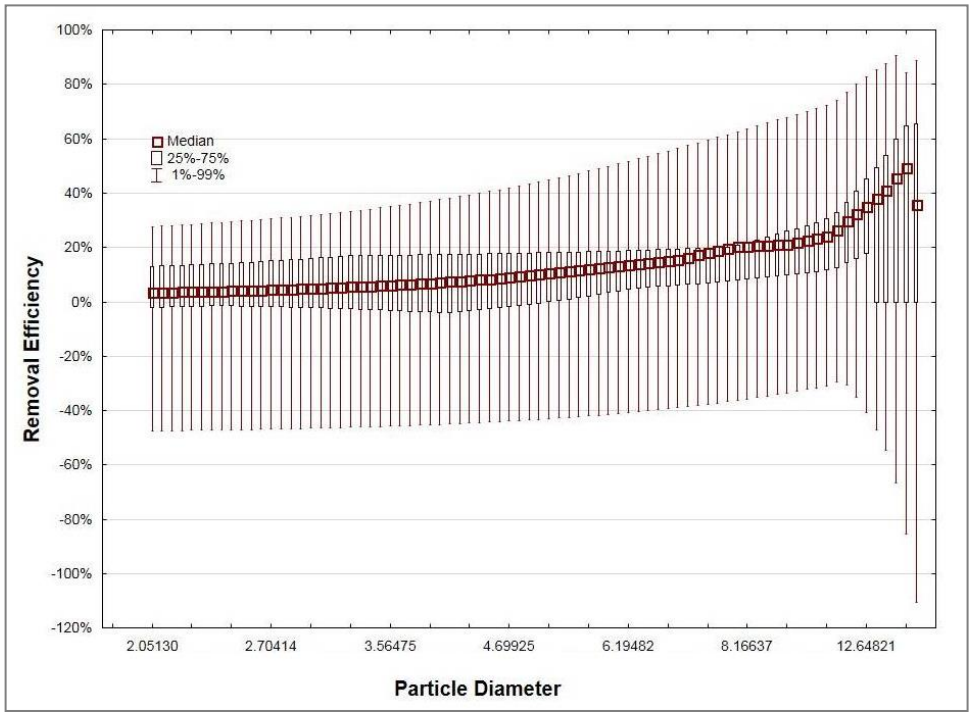


Figure 3.8 Removal Efficiency for 20 µm GE filters - All Experiments

Appendix G includes individual particle removal efficiency graphs. Overall, the prototype filters showed superior particle reduction when compared to the GE control filters.

### 3.1.3 Micrographs

The SEM analyses of filter surfaces of several test filters clearly show clogging from particles. Appendix D includes all micrograph analyses provided by the test cartridge supplier.

## 3.2 Hydraulic Performance

Hydraulic performance comparison was observed using specific flux, pressure drop (ΔP), the Cartridge Filter Fouling Index (CFFI), and run time duration.

### 3.2.1 Flux

Figure 3.9 shows a general decrease in specific flux with decrease in porosity. The G filter which is like a 15 µm C filter on the inside and a 25 µm A filter on the outside showed flux performance to be between that of the A and C filters.

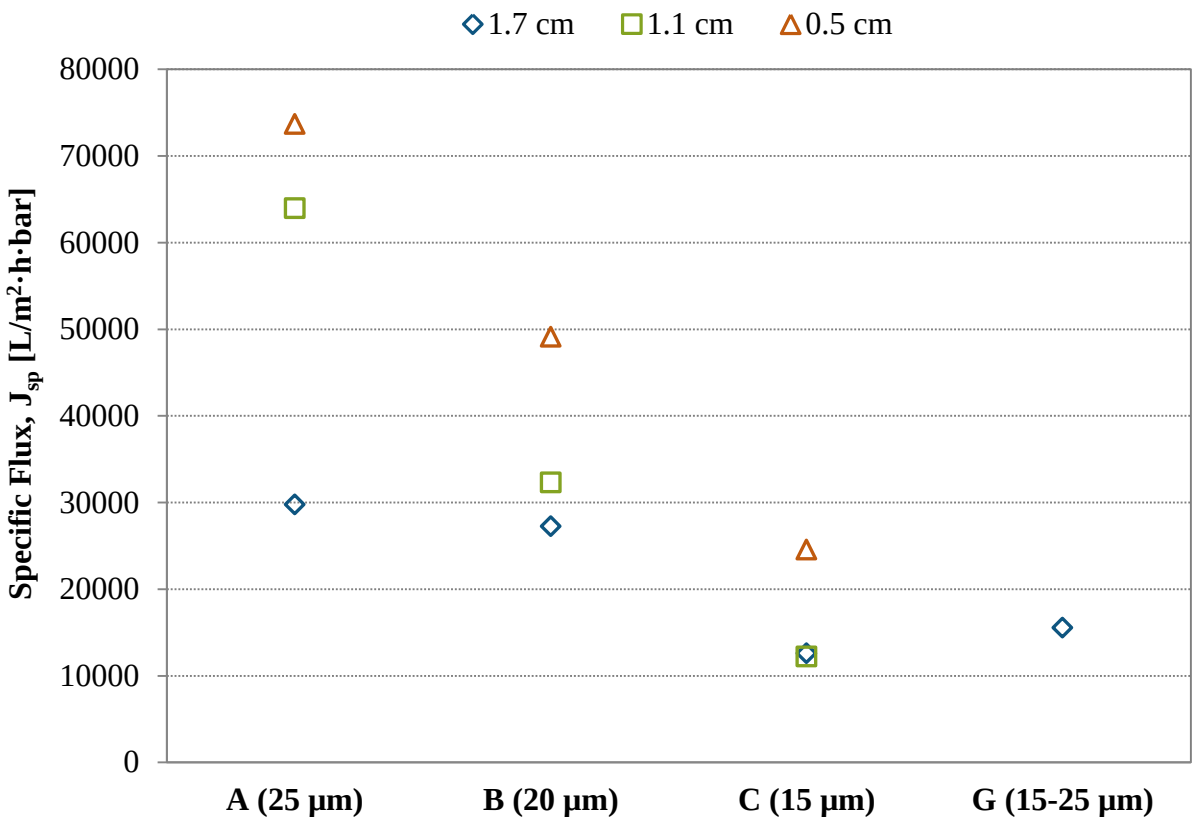


Figure 3.9 Prototype Filter - Specific Flux

### 3.2.2 Pressure Drop

Excluding the test filters which collapsed or performed poorly (A2, B2, E1, F1-50%), as well as those where the pressure drop data was not recorded or suspect (C2), the best performing test filters include the D1, F1, and A1, all of which had a clean membrane differential pressure less than 4 psi. Figure 3.10 summarizes the average test filter pressure drop data.

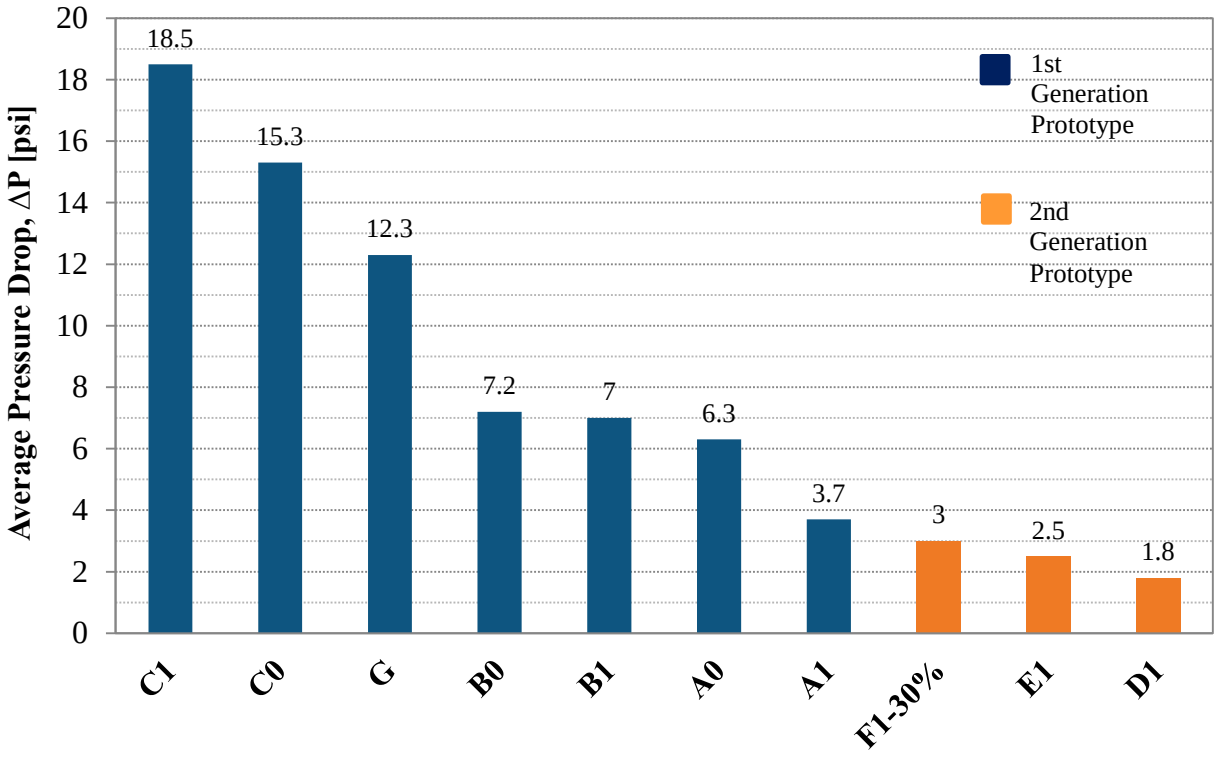


Figure 3.10 Average Test Filter Pressure Drop (EPWU Finished Water)

### 3.2.3 Cartridge Filter Fouling Index (CFFI)

The A2 and B2 filters collapsed and were eliminated from comparison. The C2 filter was considered suspect. From Figure 3.11, data for the A1, B1 and C1 filters indicate high CFFI. Higher CFFI is indicative of a higher fouling rate, which coincides with decrease in pore size.

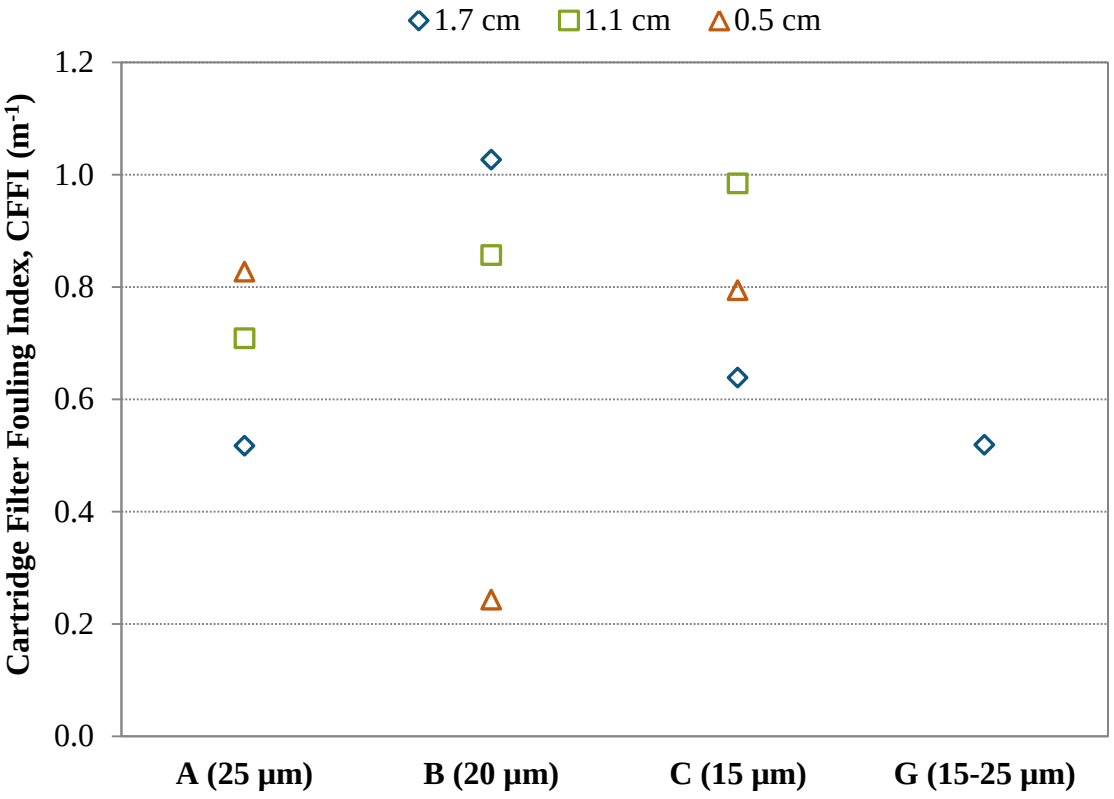


Figure 3.11 Prototype Filter - Cartridge Filter Fouling Index (CFFI)

### 3.2.4 Run Time Duration (periodicity/backwash frequency)

The silica slurry filter run time is an indication of the performance of each Test filter in treating water of poor quality (i.e. high suspended solids/NTU). Excluding the filters that collapsed or did not remove turbidity reliably (F1-50%, A2, B2, E1-I), the G, A, and D1 filters all performed well. Each had a run time at or above 59 minutes. The F1-30% had a lower overall run time (46.5 minutes). Since it has such a low clean water pressure drop and good particle reduction, the F1-30% should be considered along with the other top performing cartridge filters. Figure 3.12 summarizes the average test filter Run 1 - run times.

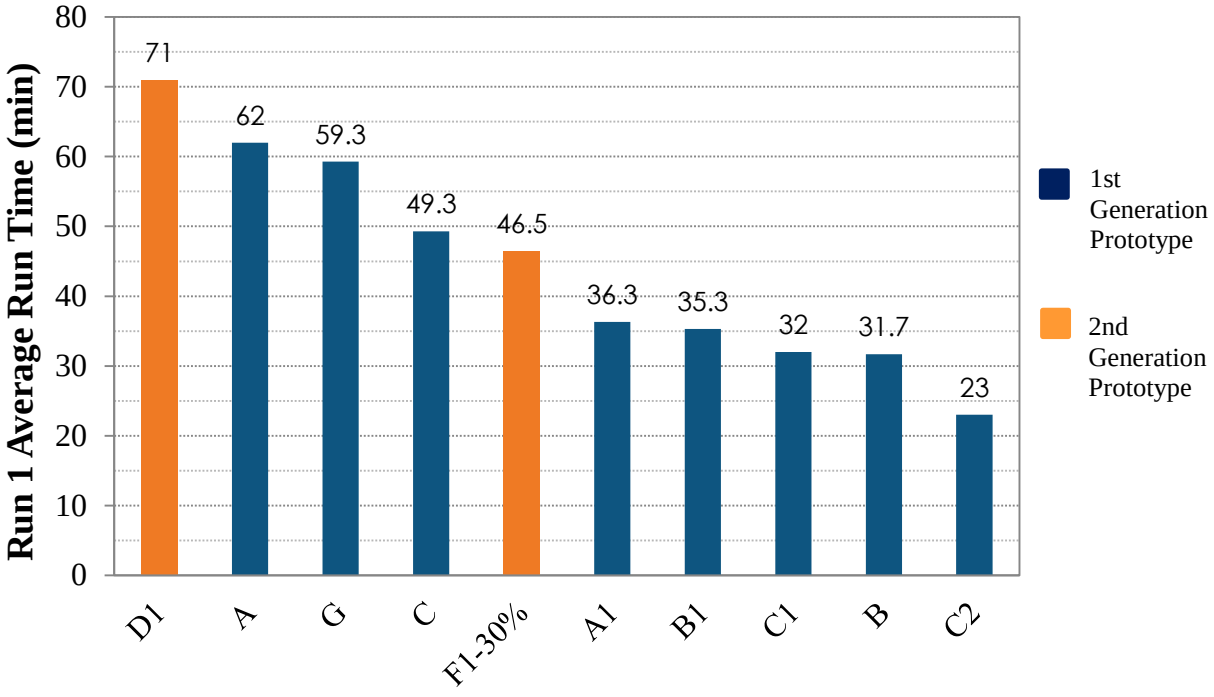


Figure 3.12 Average Test Filter Run Time

# Chapter 4: Conclusions

## First Generation Prototypes

The prototype test filters (A, B and C) performed substantially better than the GE control filters, in terms of particle reduction and backwashability. All prototype filters (excluding those that collapsed) had consistently reduced turbidity and particle concentrations. There was not a strong correlation between wall thickness and particle reduction, but pore size showed a clear correlation. Smaller pore size was indicative of higher particle reduction but also higher fouling rates. The A2 and B2 filters, with wall thickness of 0.5 cm, collapsed. The A filter showed a wider range of performance after backwashing; this may be due to varied turbidity of the feedwater. The G filter showed the most consistency in performance.

## Second Generation Prototypes

The second generation prototype filter designs (D1, E1, and F1) had improved operational characteristics (with the exception of the F1-50% filters), in that they had similar pressure drops as compared to the GE control filters. They did show lower particle reductions than the original prototypes, but reductions were still higher than those of the GE control filters. The D1 and F1-30% filters required substantially lower feed pressures, and it is reasonable to expect that longer run times could be possible with a lower applied feed pressure.

## Overview of Test Filters

All of the test filters (that did not collapse) showed reliability in particle reduction. All of the test filters seem to have an effective pore size smaller than the average pore size (based on mercury intrusion) provided by the supplier. The prototype cartridge filters showed turbidity reductions greater than 97%. On average, the A, D1, F1-30%, and G filters removed 98-99% of the particles greater than 5 microns. The best filters, in terms of the performance metrics of pressure drop, run length, and particle reduction, are the A, G, D1, and F1-30% cartridge filters.

**Cost Implications**

A qualitative evaluation of the prototype and second-generation filters, summarized in Table 4.1, can be made in terms of filter cost comparisons:

- Filters with larger wall thickness may cost more than filters with thinner walls due to the extra material needed in making the larger filter.
- Filters with more intricate matrices, such as the F1-30% and 50% filters and the G filter, may require additional manufacturing/processing, which will likely increase costs.
- Backwashable filters compared to typical single-use filters will need to be changed out less frequently and reduce filter replacement costs.
- Filters requiring higher feed pressures will increase plant costs compared to those that can operate at lower pressure.
- Filters with higher CFFI's may foul quickly and require more frequent backwashing or replacement, likely increasing costs.

Table 4.1 General Cost Assumptions

| | | |
|---|---|---|
| ⇧ Material | = | ⇧ Filter Cost |
| ⇧ Manufacturing Complexity | = | ⇧ Filter Cost |
| ⇩ Replacement Frequency | = | ⇩ Replacement Cost |
| ⇩ Feed Pressure | = | ⇩ Operational Cost |

**Further Research**

The majority of the test filters observed in this study are capable of being backwashed. With further testing, the backwashability of the filters can be analyzed for optimization. For example, online turbiditmeters could be used to optimize the flux and pulsatile flow conditions of the backwash. Also, modifications could be made to the cartridge filter housing to allow solids to be flushed downwards. Testing of possible third generation prototypes may lead to increased optimization of filter hydraulic performance and particle removal efficiency.

# References


Alhadidi, A., Kemperman, A., Schippers, J., Wessling, M., & van der Meer, W. (2011). The influence of membrane properties on the silt density index. *Journal of Membrane Science, 384*(1-2), 205-218. doi:10.1016/j.memsci.2011.09.028

ASTM Standard. (2007). D4189-07. *Standard Test Method for Silt Density Index (SDI) of Water*. West Conshohocken, PA: ASTM International. doi:10.1520/D4189-07

Bentley, J., & Lloyd, P. (1992, July-August). Interpreting the rating of cartridge filters. *Filtration & Separation, 29*(4), 333-335.

Boerlag, S. F., Kennedy, M. D., Bonne, P. A., Galjaard, G., & Schippers, J. C. (1997). Prediction of flux decline in membrane systems due to particulate fouling. *Desalination, 113*(2-3), 231-233. doi:10.1016/S0011-9164(97)00134-3

Bonnelye, V., Sanz, M. A., Durand, J.-P., Plasse, L., Gueguen, F., & Mazounie, P. (2004). Reverse osmosis on open intake seawater: pre-treatment strategy. *Desalination, 167*, 191-200. doi:10.1016/j.desal.2004.06.128

Buehner, F. (2009). Estimating the Total Cost of Cartridge and Bag Filtration. *Chemical Engineering, 116*(10), 34-43. Retrieved March 04, 2013, from http://www.wesellfans.com/pdf/Catridge_vs_Bag.pdf

Bu-Rashid, K. A., & Czolkoss, W. (2007). Pilot Tests of Multibore UF Membrane at Addur SWRO Desalination Plant, Bahrain. *Desalination, 203*(1-3), 229-242. doi:10.1016/j.desal.2006.04.010

Desormeaux, E. (2009). Pilot Plant Testing Results: swcd2 Informational Meeting (slide 5).

El Paso Water Utilities. (2007). *Public Information*. Retrieved from http://www.epwu.org/public_info/tech2o.html

Fritzmann, C., Lowenberg, J., Wintgens, T., & Melin, T. (2007). State-of-the-art of reverse osmosis desalination. *Desalination, 216*(1-3), 1-76. doi:10.1016/j.desal.2006.12.009

Gleick, P. (2006). The World's Water 2006-2007. *The Biennial Report on Freshwater Resources*. Island Press, Chicago.

Greenlee, L. F., Lawler, D. F., Freeman, B. D., Marrot, B., & Moulin, P. (2009). Reverse osmosis desalination: Water sources, technology, and today's challenges. *Water Research, 43*(9), 2317-2348. doi:10.1016/j.watres.2009.03.010

GWI. (2012, 10 1). *Latest desal plant inventory released.* Retrieved 1 29, 2013, from GWI Water Desalination Report: http://www.desalination.com/wdr/48/38/latest-desal-plant-inventory-released

ISO. (1981). *ISO Standards.* Retrieved 6 7, 2012 (Withdrawn), from ISO 4572:1981 Hydraulic fluid power - Filters - Multi-pass method for evaluating filtration performance: http://www.iso.org/iso/iso_catalogue/catalogue_ics/catalogue_detail_ics.htm?csnumber=10494

ISO. (2008). *ISO Standards.* Retrieved from ISO 16889:2008 Hydraulic fluid power -- Filters -- Multi-pass method for evaluating filtration performance of a filter element: http://www.iso.org/iso/iso_catalogue/catalogue_tc/catalogue_detail.htm?csnumber=44870

Jourdan, M., Peuchot, C., & Hunt, T. (1994, July-August). New test method for evaulation of water cartridge filters. *Filtration & Separation, 31*(5), 247-434.

Kremen, S. S., & Tanner, M. (1998). Silt density indices (SDI), percent plugging factor (%PF): their relation to actual foulant deposition. *Desalination, 119*(1-30), 259-262. doi:10.1016/S0011-9164(98)00167-2

Moran, Y., Schreiber, E., Skelly, J., & Volpe, D. (2010, April 19). Green reverse osmosis pretreatment for shipboard desalination. Retrieved March 10, 2013, from http://www.wpi.edu/Pubs/E-project/Available/E-project-042710-161430/unrestricted/GreenReverseOsmosisPretreatment.pdf

Mosset, A., Bonnelye, V., Petry, M., & Sanz, M. A. (2008). The sensitivity of SDI analysis: from RO feed water to raw water. *Desalination, 222*(1-3), 17-23. doi:10.1016/j.desal.2007.01.125

MWH. (2012). *Water Treatment princliples and design* (3 ed.). (J. C. Crittenden, R. R. Trussell, D. W. Hand, K. J. Howe, & G. Tchobanoglous, Eds.) New Jersey: John Wiley & Sons, Inc.

Nason, J. A. (2006). Particle aspects of precipitative softening: experimental measurement and mathematical modeling of simultaneous precipitation and flocculation. 56-57. Retrieved March 28, 2013, from http://repositories.lib.utexas.edu/bitstream/handle/2152/2835/nasonj96987.pdf?sequence=2

NIST. (2011a, August 19). *Material Measurement Laboratory.* Retrieved 6 7, 2012, from Report of Investigation: RM 8631a - Medium Test Dust (MTD): https://www-s.nist.gov/srmors/view_report.cfm?srm=8631a

NIST. (2011b, August 19). *Material Measurement Laboratory: Standard Reference Materials.* Retrieved 6 7, 2012, from Report of Investigation: RM 8632 - Ultra Fine Dust: https://www-s.nist.gov/srmors/view_report.cfm?srm=8632

Park, C., Kim, H., Hong, S., & Choi, S. (2006). Variation and prediction of membrane fouling index under various feedwater characteristics. *Journal of Membrane Science, 284*(1-2), 248-254. doi:10.1016/j.memsci.2006.07.036

Peuchot, C., Petillon, N., & Lynch, J. (2008). Filter efficiency and liquids: The advantages of cartridge filters. *Filtration & Separation, 45*, 11-13. doi:10.1016/S0015-1882(08)70386-0

Porex Filtration Division. (2013). Retrieved from http://www.porexfiltration.com/

Rybar, V. S., Vodnar, M., Vartolomei, F. L., Mendez, R. L., & Ruano, J. L. (2005). Experience with Renewable Energy Source and SWRO Desalination in Gran Canaria. International Desalination Association World Congress. Retrieved May 11, 2013, from http://www.membranes.com/docs/papers/New%20Folder/Soslaires%20Canarias%20Desalination%20Plant.pdf

Schippers, J. C., & Verdouw, J. (1980). The modified fouling index, a method of determining the fouling characteristics of water. *Desalination, 32*, 137-148. doi:10.1016/S0011-9164(00)86014-2

Sutherland, K. (2009). Filtration & Separation Technology: Whats new with Cartridge Filters . *Filtration & Separation, 46*(2), 34-36. doi:10.1016/S0015-1882(09)70037-0

Tsiourtis, N. X. (2001). Desalination and the environment. *Desalination, 141*(3), 223-236. doi:10.1016/S0011-9164(01)85001-3

US Silica. (2013). Retrieved from http://ussilica.com

Vijlee, A. (2002, November). *Machinery Lubrication.* Retrieved June 7, 2012, from Standardized Test Dusts - ACFTD vs. ISO MTD: http://www.machinerylubrication.com/Read/418/test-dust-ACFTD

Voutchkov, N. (2010). Considerations for selection of seawater filtration pretreatment system. *Desalination, 261*(3), 354-364. doi:10.1016/j.desal.2010.07.002

Wilf, M., & Bartels, C. (2006). Integrated membrane desalination systems - current status and projected development. *Hydranautics*. Retrieved May 11, 2013, from http://www.membranes.com/docs/papers/New%20Folder/Abstract%20for%20Tianjin%20-%20Hydranautics.pdf

Williams, C. (1992, March-April). Testing the Performance of Spool-Wound Cartridge Filters. *Filtration & Separation, 29*(2), 162-168. doi:10.1016/0015-1882(92)80045-K

Williams, C. (1997). The case for a new European standard designation for process cartridge filter efficiency. *Filtration & Separation, 34*(5), 459-462. doi:10.1016/S0015-1882(97)84753-2

Williams, C., & Edyvean, R. (1995, March). Testing cartridge filters in aqueous media: interpreting the results - the pitfalls and problems (Part 2: The problems and pitfalls of cartridge filter performance evaluation). *Filtration & Separation, 32*(3), 255-259. doi:10.1016/S0015-1882(97)84050-5

Williams, C., & Edyvean, R. (1996). The effect of organically loaded feedstreams on the operation of cartridge filters. *Water Resouces, 30*(4), 972-980. doi:10.1016/0043-1354(95)00244-8

Zhou, Y., & Tol, R. S. (2005). Evaluating the costs of desalination and water transport. *Water Resources Research, 41*(3). doi:10.1029/2004WR003749

# Appendix A – GE Hytrex Specifications

GE Power & Water
Water & Process Technologies

**Fact Sheet**

# Hytrex*

## Depth Cartridge Filters

**Figure 1 : Hytrex Depth Cartridge Filters**

### Description and Use

The purity and reliability of Hytrex* cartridge filters (Figure 1) ensure consistent results, time after time. Thermally bonded micro fibers create a strong secure cartridge that traps particles throughout its depth. Hytrex combines efficiency, long life and purity to create a high performance depth filter.

- Pure polypropylene construction
- Fast rinse-up in high purity applications
- Meets the requirement of the FDA Title 21 of the Code of Federal Regulations 174.5 and relevant subparts of 177
- Wide chemical compatibility
- Automated packaging for a clean finished product
- NSF Standard 42 certified

### Typical Applications

- High Purity Chemicals
- Bottled Water
- Pre-treatment for Reverse Osmosis
- Oil & Gas
- Electronics

### Consistent Performance

Patented, continuous process assures consistent product performance. Lot-to-lot, order-to-order, strict quality control assures repeatability. Figures 2 and 3 give greater detail of the high flow rate at low pressure drop for the various sizes of Hytrex filters.

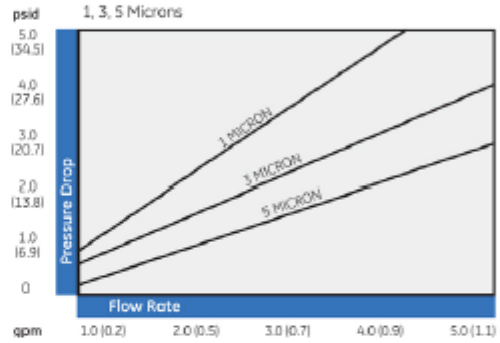


**Figure 2: High Flow Rate at Low Pressure Drop[1]**

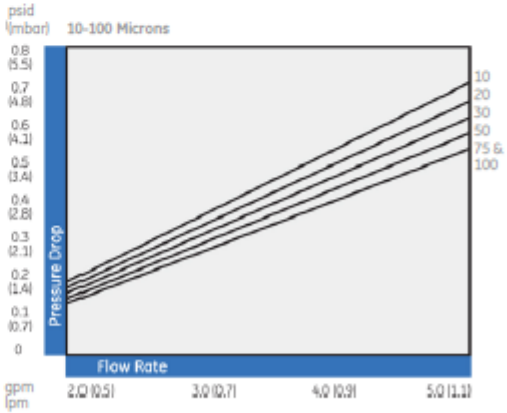


**Figure 3: High Flow Rate at Low Pressure Drop[1]**

[1] Data based on 10" length filter with clean water.

Find a contact near you by visiting www.ge.com/water and clicking on "Contact Us".



FS1074EN.doc Aug-10

## Operating Pressure & Temperature

- Maximum operating differential pressure: 35 psid @ 100°F (38°C)
- Maximum operating temperature: 160°F (71°C) @ 15 psid (103.4 kPa)

## High Dirt Holding Capacity

- True-graded density captures particles throughout entire filter depth
- High dirt-holding capacity means longer life and fewer changeouts which translates to money saved
- Lower density at the surface of the filter with progressively higher density toward the center
- No surface blinding, which reduces flow and increases filter changeouts

## Wide Range of Lengths & Adapters

- Standard lengths fit most housings—custom lengths can also be provided
- Wide range of polypropylene end-adapters including gaskets, extended cores and
- GE patented self-seal polypropylene springs
- If required, specify FDA-compliant sealing materials and end adapters
- Table 1 details specific ordering information.

## Material and FDA Compliance

Hytrex cartridge filters are made from thermally-welded blown microfibers of polypropylene. GE certifies that the resin used for manufacturing the filter media of this product meets the requirements of the Food and Drug Administration (FDA) Title 21 of the Code of Federal Regulations (CFR) 174.5 and relevant subparts of 177. If required, specify FDA-compliant sealing materials and end adapters.

## Important Notice To User

The following is made in lieu of all other warranties expressed or implied. Manufacturer's and Seller's only obligation shall be to issue credit against the purchase or replacement of the product proved to be defective in material or workmanship. Neither Manufacturer nor Seller shall be liable for any injury, loss or damage, direct or indirect, special or consequential, arising out of the use of, misuse, or the inability to use such product. The information contained herein is based on technical data and tests which we believe to be reliable and is intended for use by persons having technical skill at their discretion and risk. Since conditions of use are outside GE control, we can assume no liability whatsoever for results obtained or damages incurred through the application of the data presented. This information is not intended as a license to operate under, or a recommendation to infringe upon, any patent of GE or others covering any material or use. The foregoing may not be altered except by a written agreement signed by officers of the Manufacturer.

**Table 1: Ordering Information**

If you are ordering Hytrex filters with standard ends (with no adapter on either end), select one designation from each of the first three columns. Your Product Order Number will look like this: GX05-29 ¼. If you are ordering Hytrex with one or more end adapters, select designations from all applicable columns. Your Product Order Number will look like this: GX05-29 ¼ WP or GX05-29 ¼ XX.

| GX | 05 | 29 ¼ | Y | Y | P |
|---|---|---|---|---|---|
| **Type** | **Micron Rating** | **Cartridge Length** | **End #1 Adapter** | **End #2 Adapter** | **Gasket Material** |
| GX<br><br>ID = 1 inch (2.5 cm)<br>OD = 2.5 inch (64 cm) | 01 = 1 µm<br>03 = 3 µm[4]<br>05 = 5 µm<br>10 = 10 µm<br>20 = 20 µm<br>30 = 30 µm<br>50 = 50 µm<br>75 = 75 µm<br>100 = 100 µm | 4 7/8 inch (12.4 cm)<br>9 ¾ inch (24.8 cm)<br>9 ⅞ inch (25.1 cm)<br>10 inch (25.4 cm)<br>19 ½ inch (49.5 cm)<br>20 inch (50.8 cm)<br>29 ¼ inch (74.3 cm)<br>30 inch (76 cm)<br>40 inch (102 cm)<br>50 inch (127 cm) | Y = 1 inch (2.54 cm) Open End Gasket<br>L = Extended Core<br>E = 222 O-Ring<br>X = Standard Hytrex Plain End (No Gasket) | Y = 1 inch (2.54 cm) Open End Gasket<br>K = Self Seal Spring<br>H = Fin<br>S = Solid End<br>X = Standard Hytrex Plain End (No Gasket) | P = Santoprene[2] (Gasket Only)<br><br>**O-Rings**<br>S = Silicone<br>E = EPDM<br>V = Viton[3]<br>B = BUNA |

[2] Santoprene is licensed to Advanced Elastomer Systems, L.P. [3] Viton is a registered trademark of DuPont.

# Appendix B – Sil-CO-Sil 106 Specifications

## Product Data

US SILICA™

# SIL-CO-SIL® 106

**GROUND SILICA**

PLANT: OTTAWA, ILLINOIS

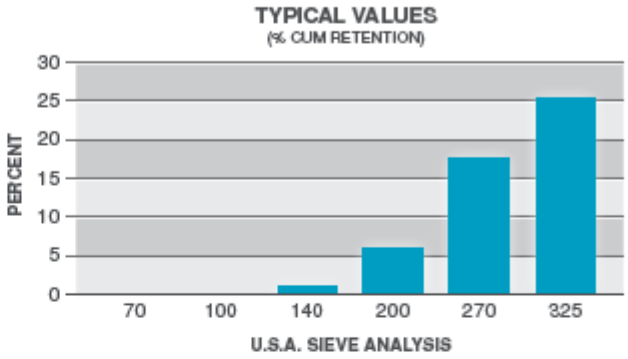


| USA STD SIEVE SIZE | | TYPICAL VALUES | | |
|---|---|---|---|---|
| | | % RETAINED | | % PASSING |
| MESH | MICRONS | INDIVIDUAL | CUMULATIVE | CUMULATIVE |
| 70 | 212 | 0.0 | 0.0 | 100.0 |
| 100 | 150 | 0.0 | 0.0 | 100.0 |
| 140 | 106 | 1.0 | 1.0 | 99.0 |
| 200 | 75 | 4.9 | 5.9 | 94.1 |
| 270 | 53 | 11.7 | 17.9 | 82.4 |
| 325 | 45 | 7.5 | 25.1 | 74.9 |

| TYPICAL PHYSICAL PROPERTIES | |
|---|---|
| Hardness (Mohs) | 7 |
| Melting Point (Degrees F) | 3100 |
| Mineral | Quartz |
| pH | 7 |
| Reflectance (%) | 79.5 |
| Yellowness Index | 4 |
| Specific Gravity | 2.65 |

| TYPICAL CHEMICAL ANALYSIS, % | |
|---|---|
| $SiO_2$ (Silicon Dioxide) | 99.7 |
| $Fe_2O_3$ (Iron Oxide) | 0.021 |
| $Al_2O_3$ (Aluminum Oxide) | 0.12 |
| $TiO_2$ (Titanium Dioxide) | 0.009 |
| CaO (Calcium Oxide) | 0.009 |
| MgO (Magnesium Oxide) | <0.01 |
| $Na_2O$ (Sodium Oxide) | <0.01 |
| $K_2O$ (Potassium Oxide) | 0.02 |
| LOI (Loss On Ignition) | 0.1 |

*April 27, 2010*


U.S. Silica Company
8490 Progress Drive, Suite 300
Frederick, MD 21701
(301) 682-0600 (phone)
(800) 243-7500 (toll-free)
ussilica.com

# Appendix C – PSD Graphs by Filter Type

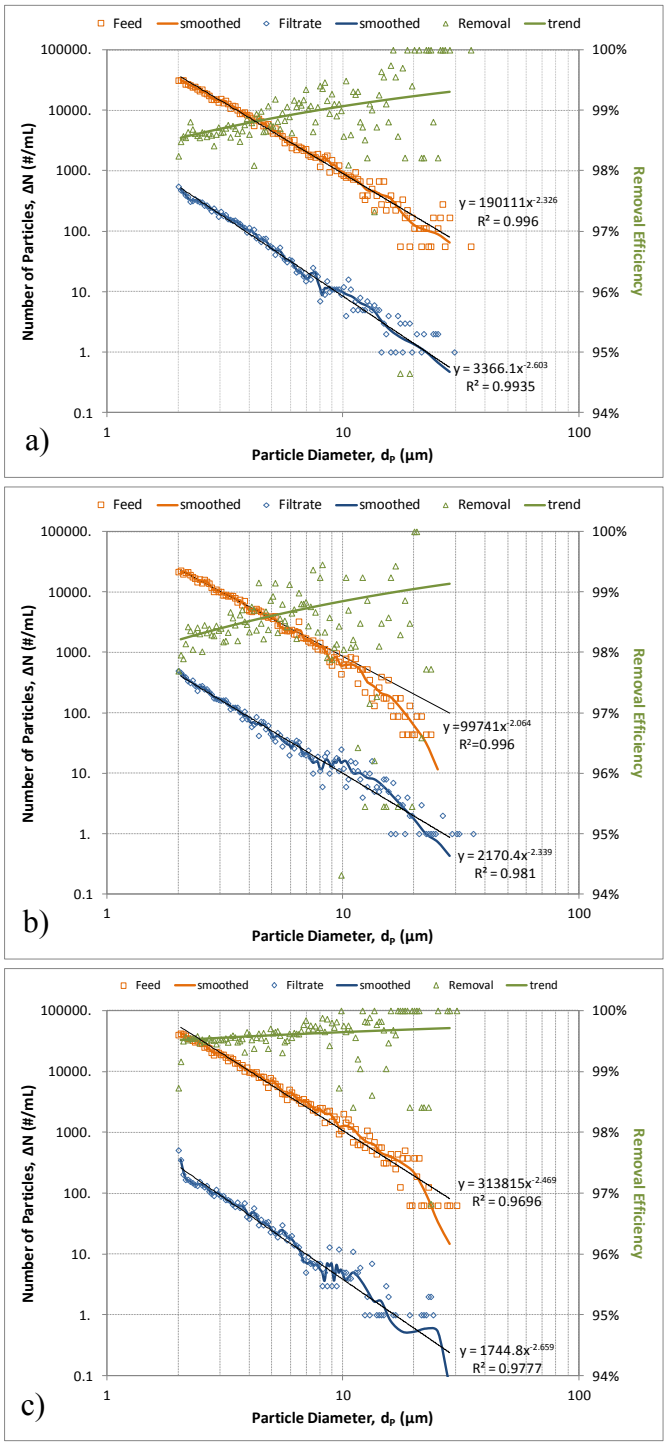


Figure C 1 Particle Removal Efficiency "A0"
Filters a) A0-1, b) A0-2, c) A0-3

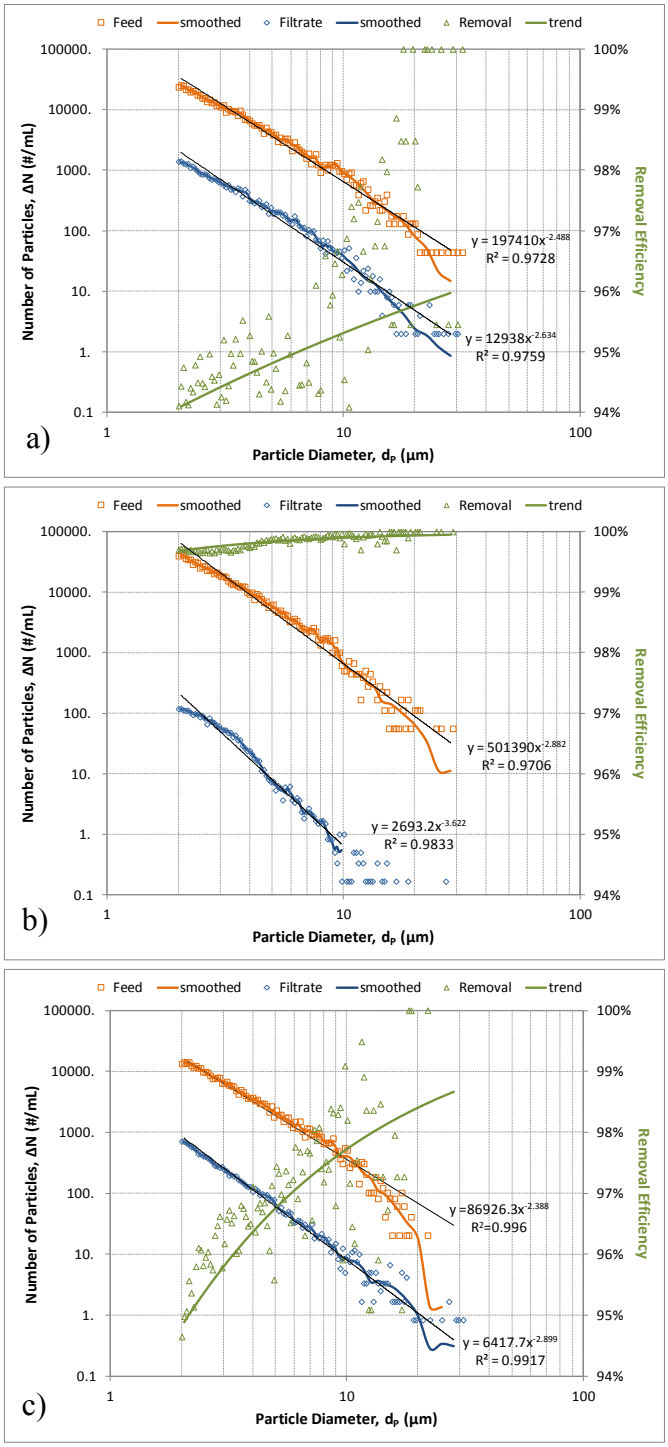


Figure C 2 Particle Removal Efficiency "A1"
Filters a) A1-1, b) A1-2, c) A1-3

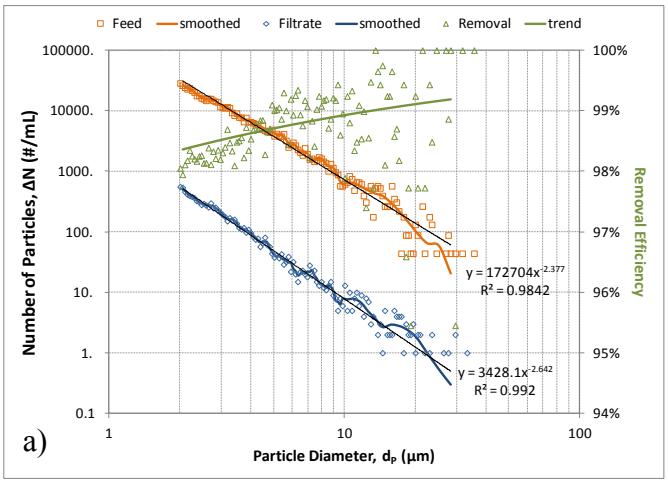


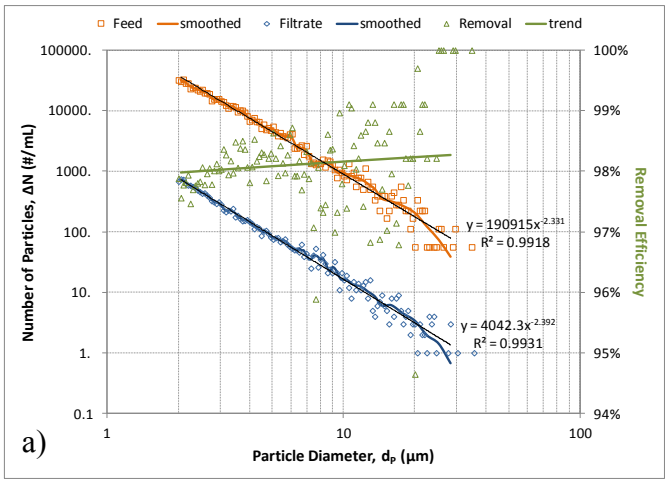


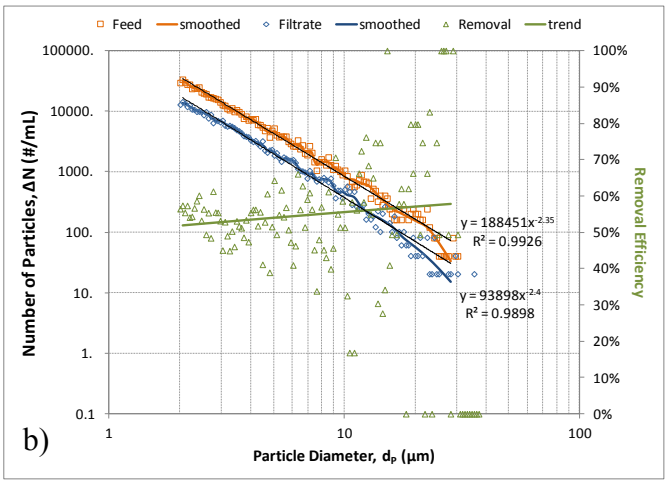


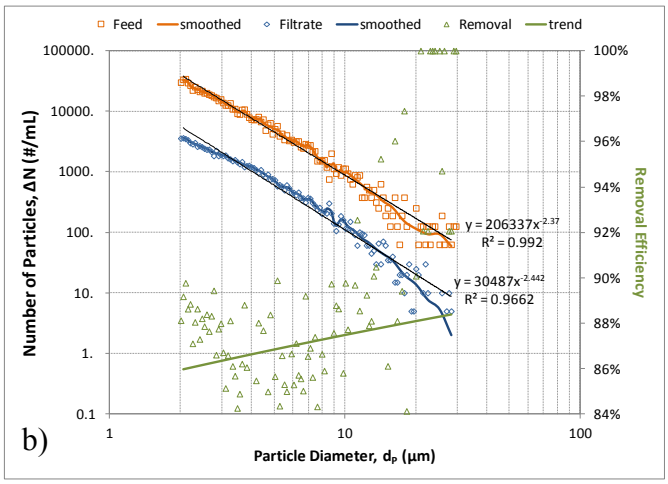


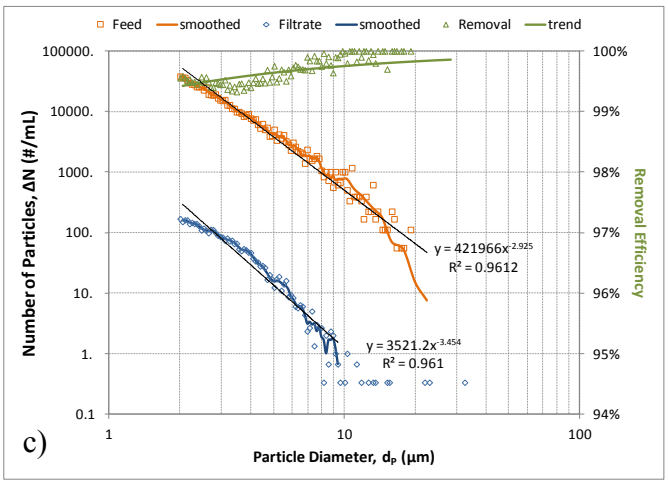


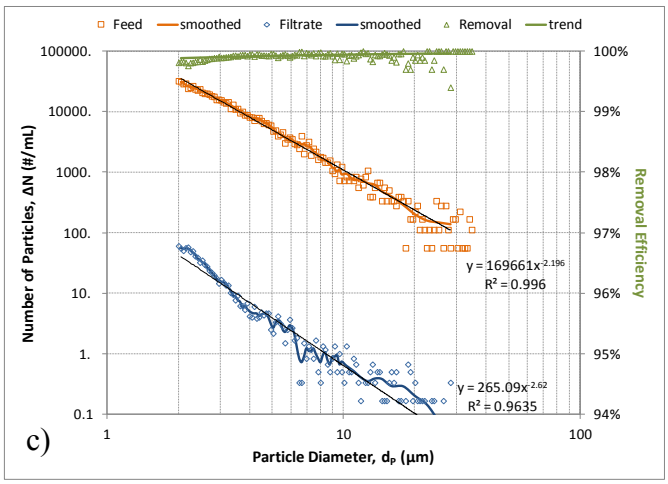


Figure C 3 Particle Removal Efficiency “A2” Filters a) A2-1, b) A2-2, c) A2-3

Figure C 4 Particle Removal Efficiency "B0" Filters a) B0-1, b) B0-2, c) B0-3

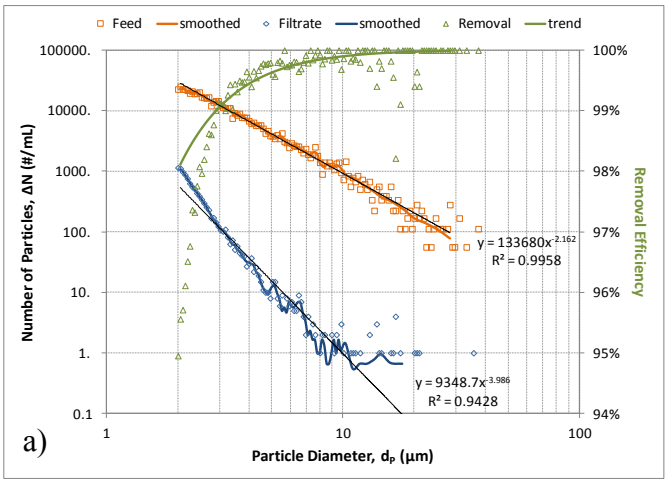


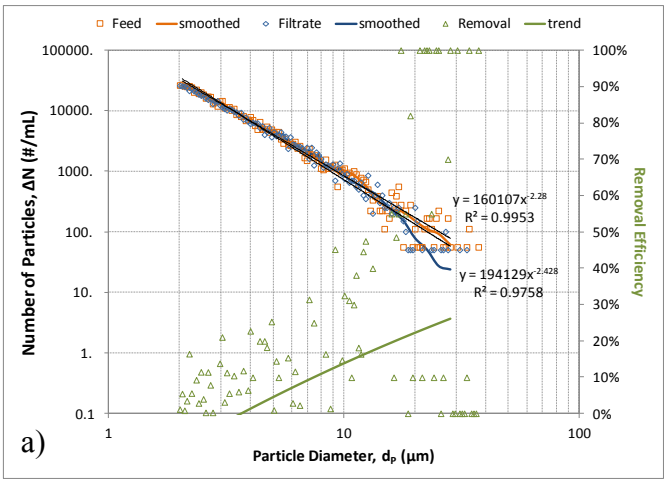


Figure C 5 Particle Size Removal Efficiency "B1" Filters a) B1-1, b) B1-2, c) B1-3

Figure C 6 Particle Size Removal Efficiency "B2" Filters a) B2-1, b) B2-2, c) B2-3

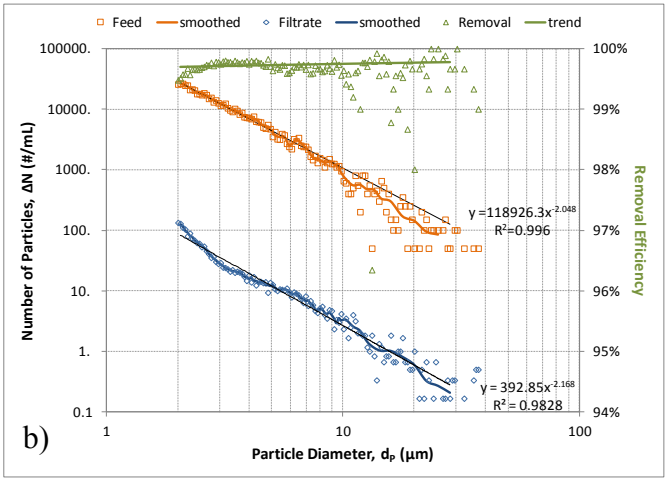


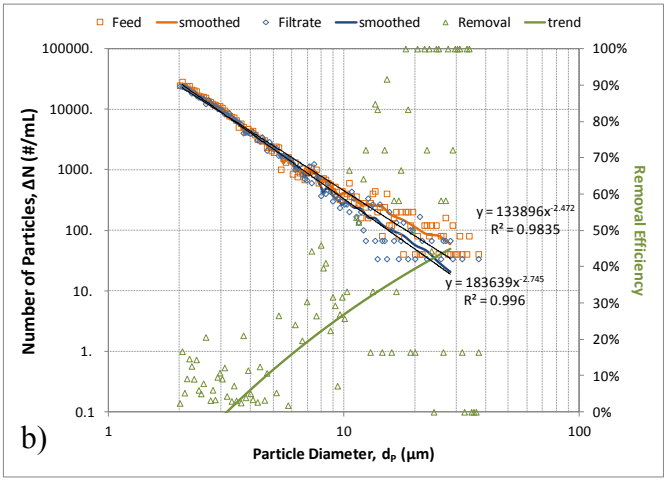


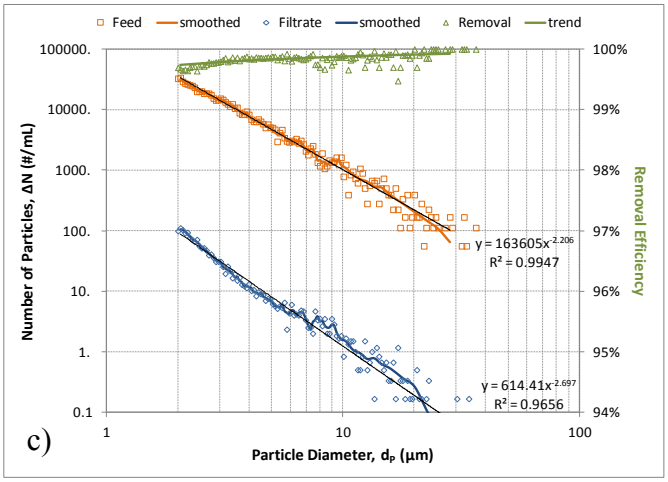


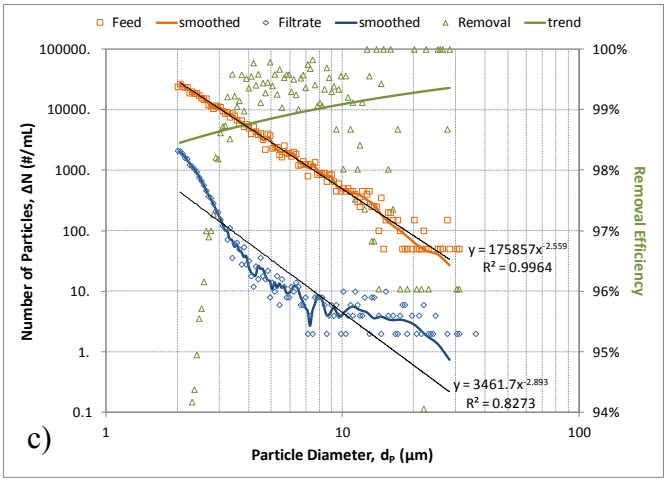

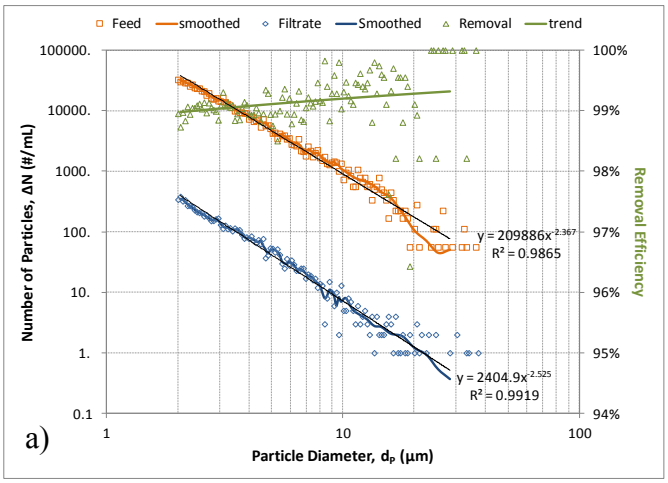


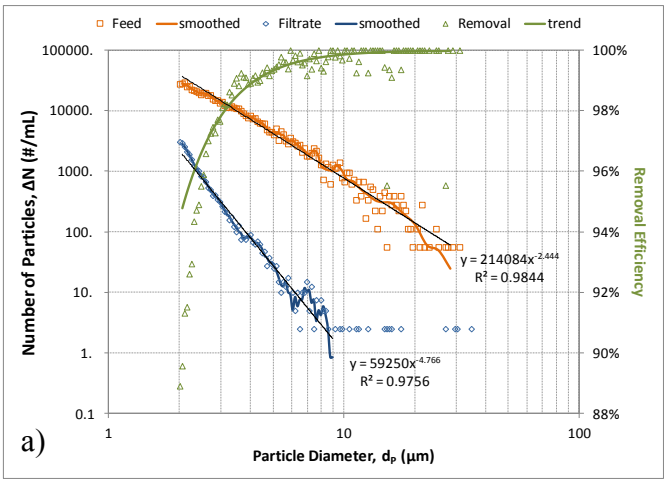


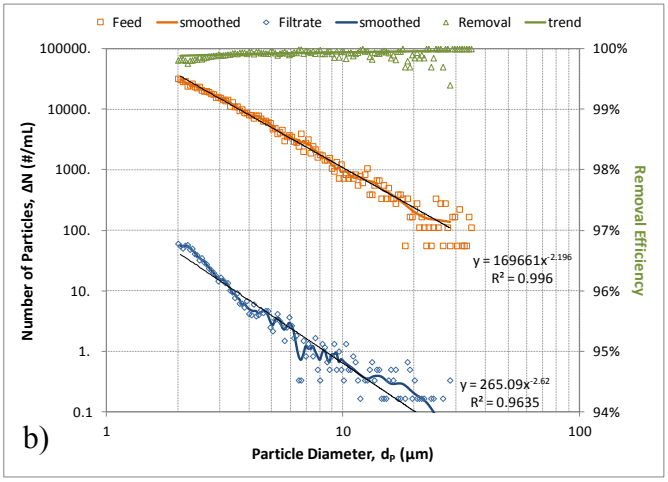


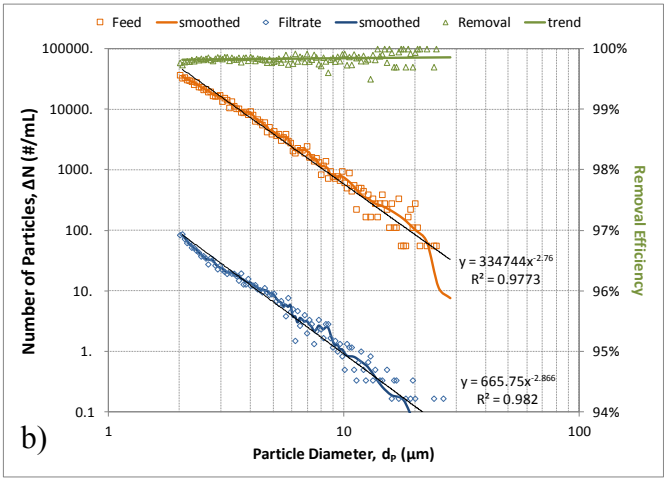


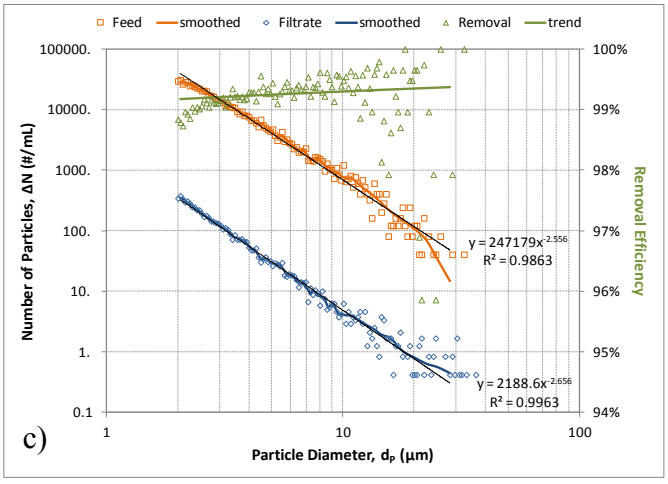


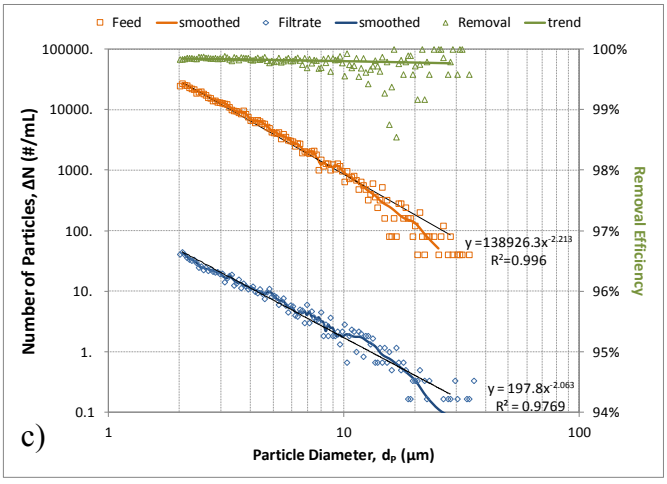


Figure C 7 Particle Size Removal Efficiency "C0" Filters a) C0-1, b) C0-2, c) C0-3

Figure C 8 Particle Size Removal Efficiency "C1" Filters a) C1-1, b) C1-2, c) C1-3

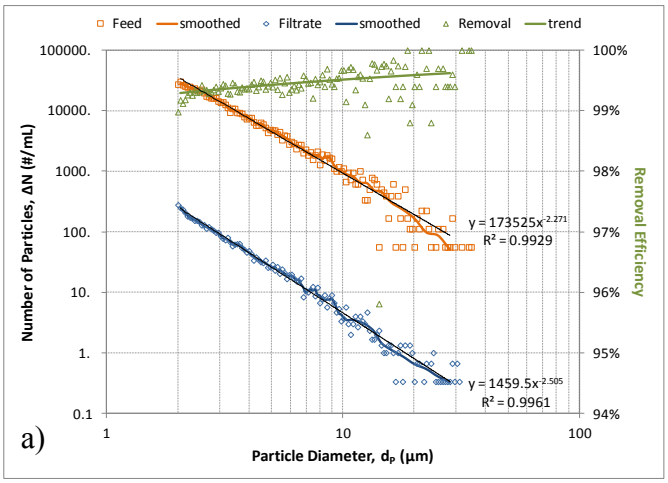


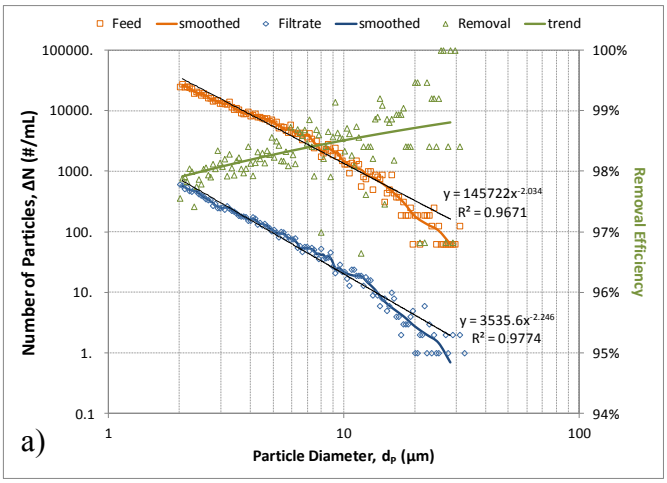


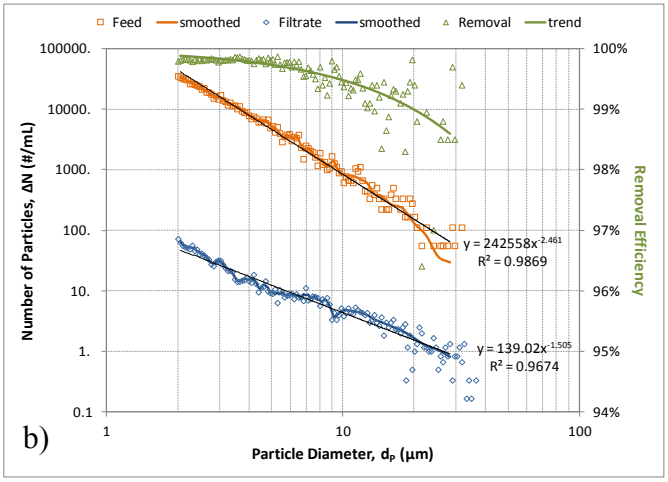


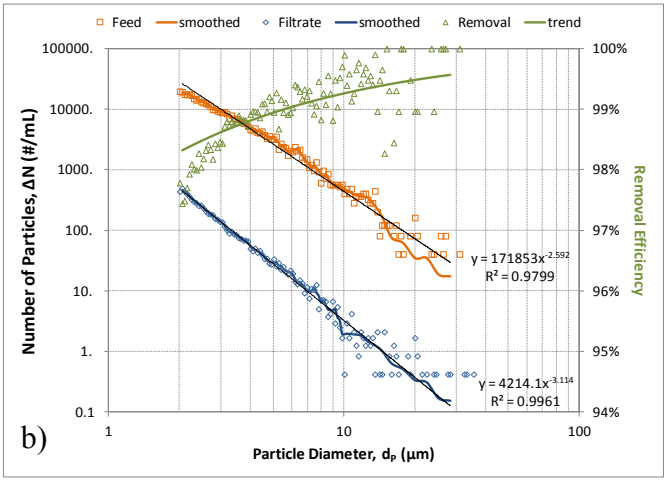


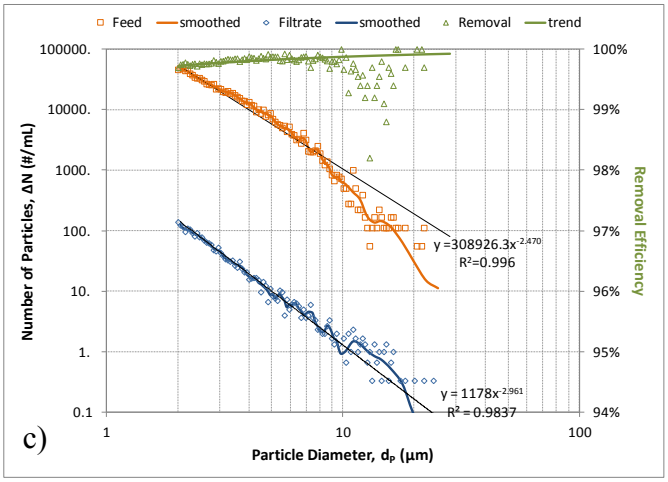


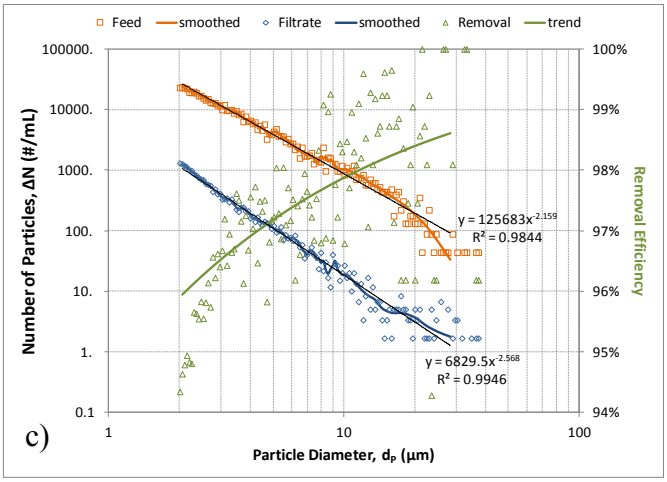


Figure C 9 Particle Size Removal Efficiency "C2" Filters a) C2-1, b) C2-2, c) C2-3

Figure C 10 Particle Size Removal Efficiency "G" Filters a) G-1, b) G-2, c) G-3

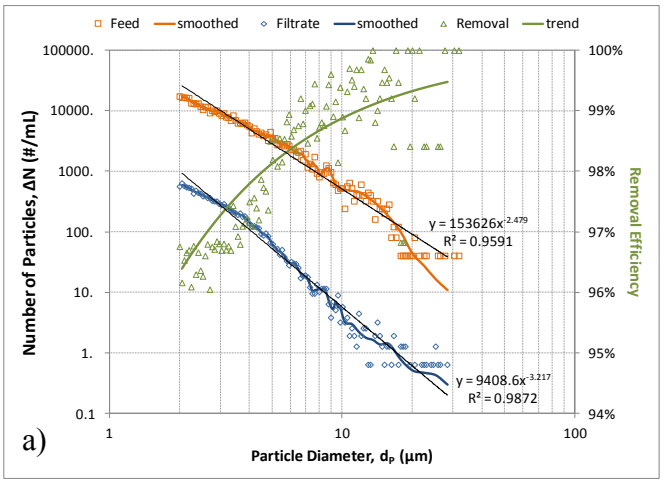


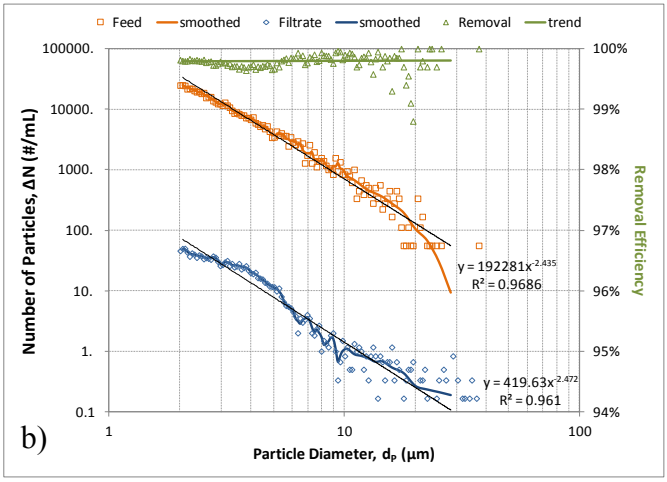


Figure C 11 Particle Size Removal Efficiency "D" Filters a) D1-I, b) D1-II

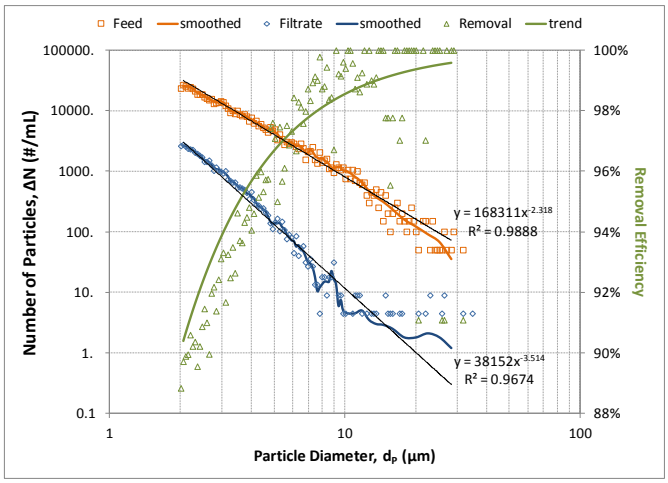


Figure C 12 Particle Size Removal Efficiency "E1-I" Filter

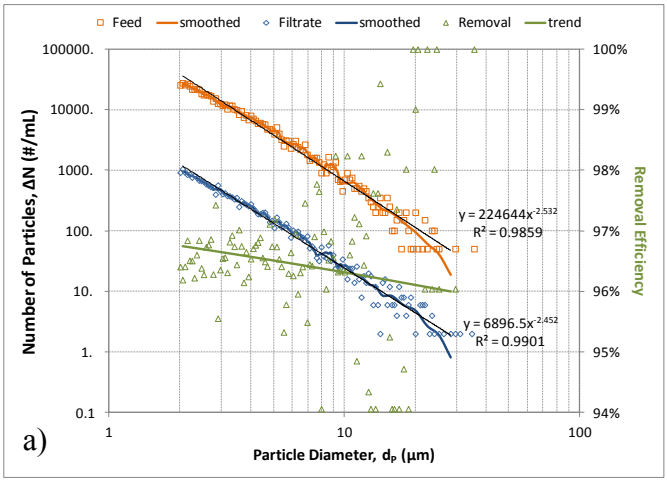


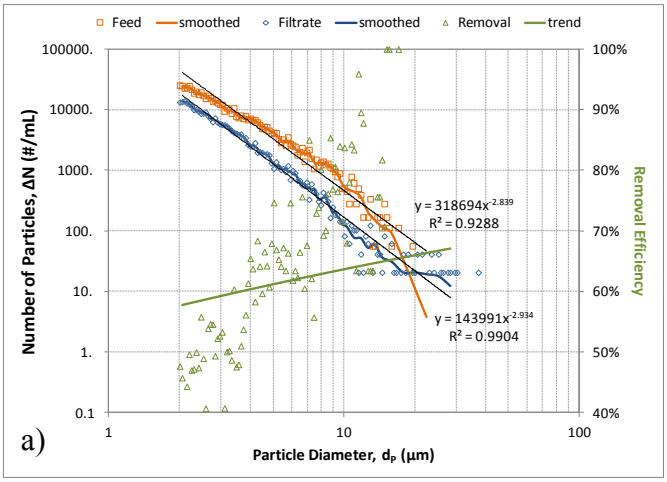


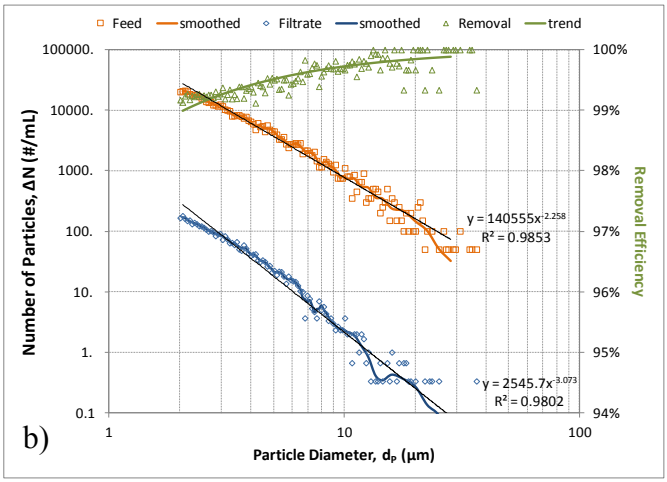


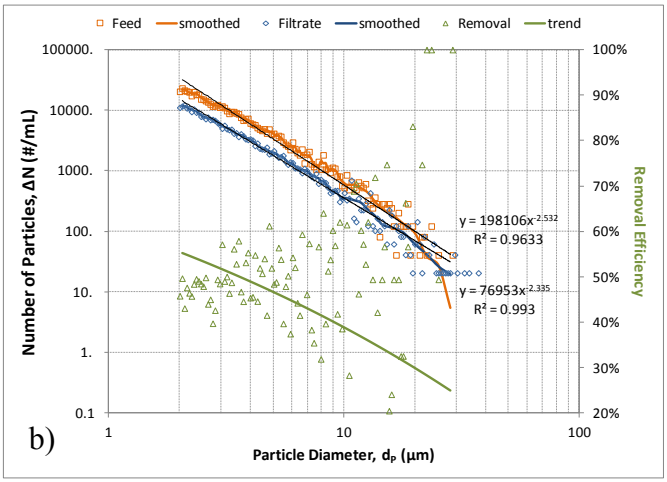


Figure C 13 Particle Size Removal Efficiency "F1-30%" Filters a) F1-30% I, b) F1-30% II

Figure C 14 Particle Size Removal Efficiency "F1-50%" Filters a) F1-50% I, b) F1-50% II

# Appendix D - Micrographs

SEM micrographs show the filter morphology, pore size, and debris trapped in the filters in representative areas

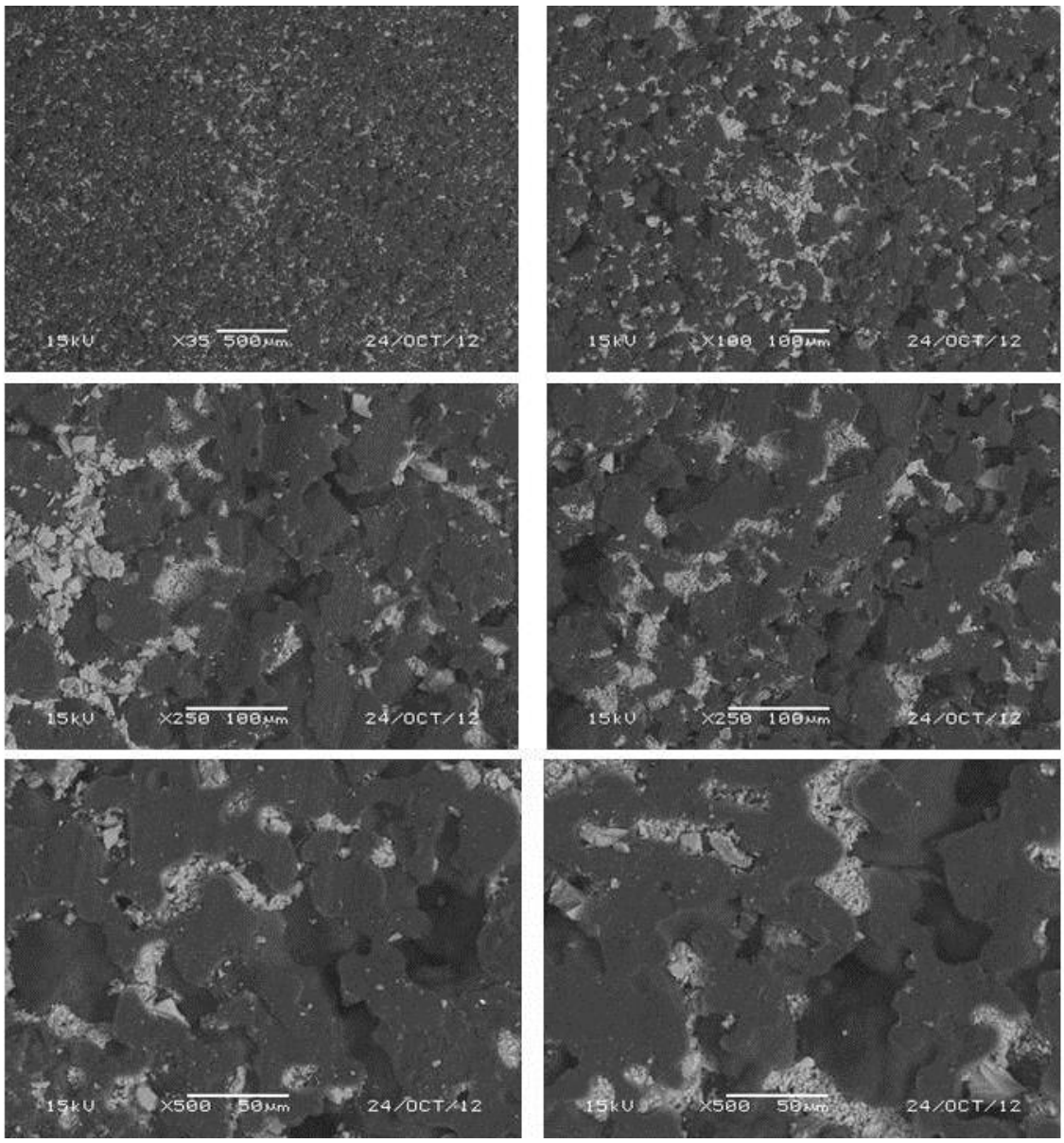


Figure D 1 Used and Backwashed "A" Filters

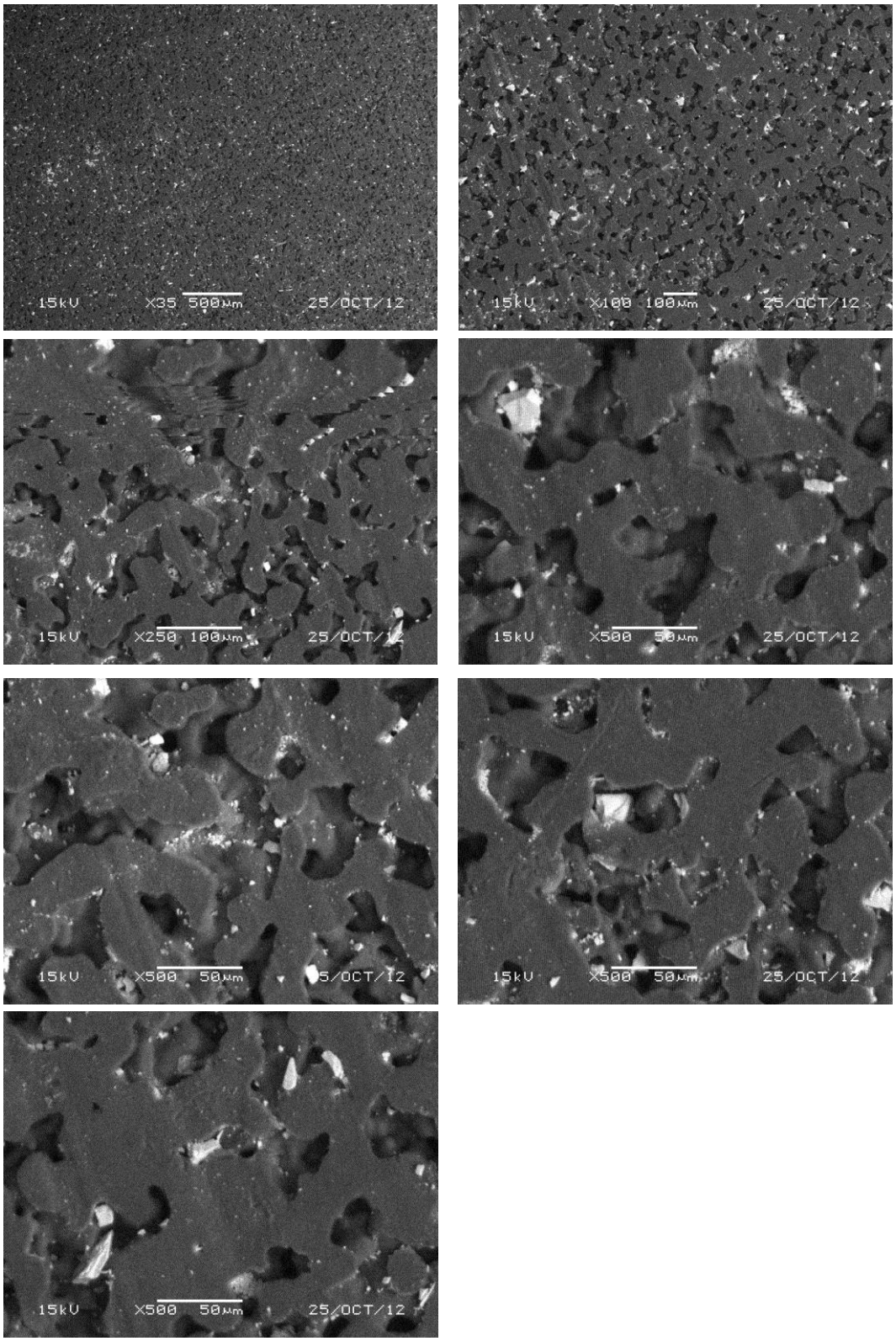


Figure D 2 Used and Backwashed "B" Filters

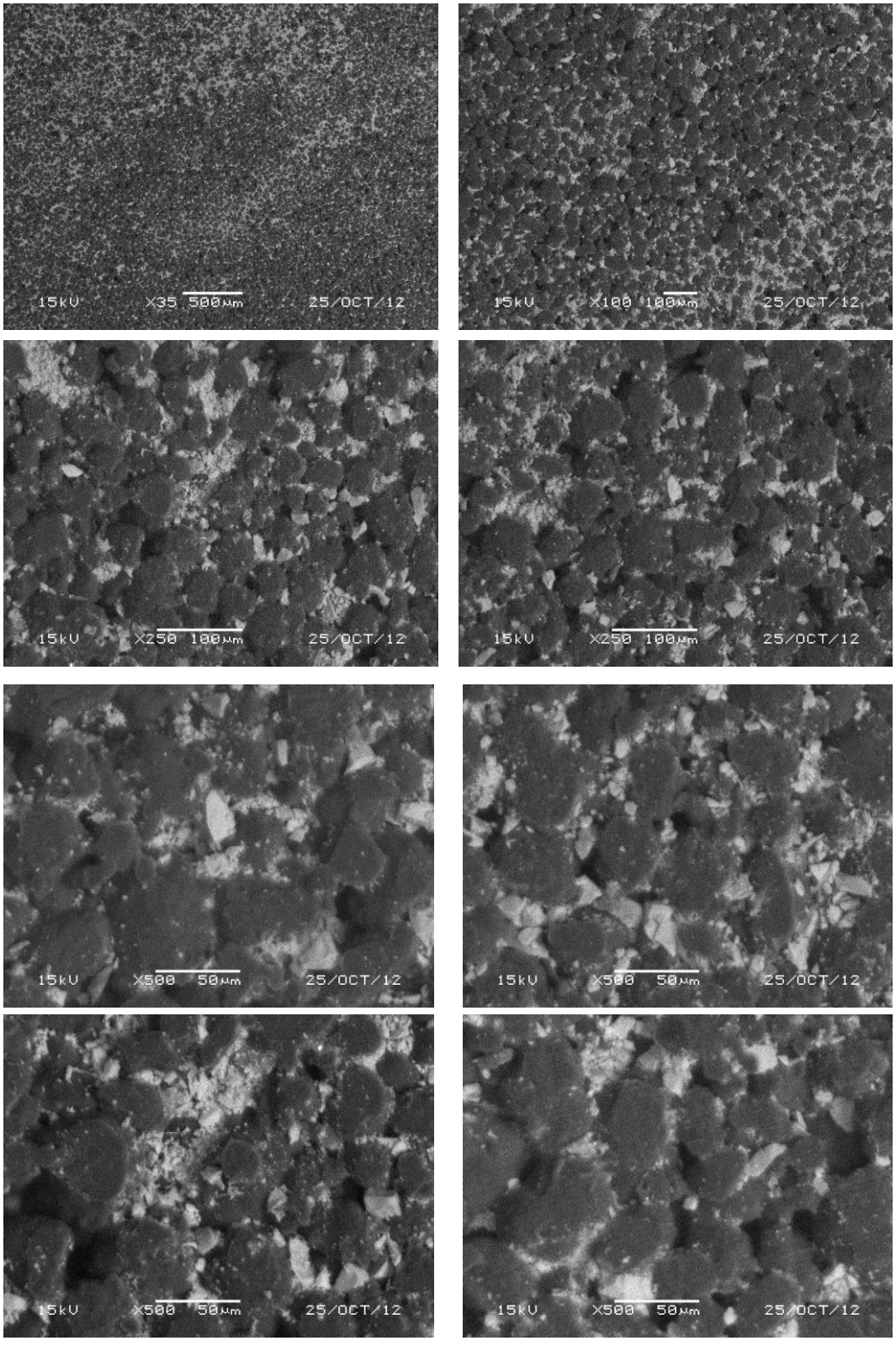


Figure D 3 Used and Backwashed "C" Filters

# Vita

Michelle Renee Brown is a native El Pasoan. She received a Bachelor of Science Degree in Metallurgical and Materials Engineering from The University of Texas at El Paso (UTEP) in 2011. As an undergraduate she had the opportunity to intern with Freeport McMoRan Copper and Gold as a metallurgist. An interest in environmental resource sustainability led her to enroll in graduate school at UTEP to begin the pursuit of a Master of Science Degree in Environmental Engineering. Michelle passed the Fundamentals of Engineering Exam while working as Graduate Research Assistant with the Center for Inland Desalination Systems (CIDS) where she learned of the different efforts to improve water desalination processes.

Permanent address: mbrown5418@gmail.com

This thesis was typed by Michelle Brown.